January 31, 2019
Revision 4 – September 6, 2019



Klamath River, California and Oregon

Topobathymetric LiDAR and Imagery Technical Data Report

Contract No. G16PC00016, Task Order 140G0218F0247

Prepared For:

USGS science for a changing world

Leslie Lansbery
USGS NGTOC
1400 Independence Rd.
Rolla, MO, 65401
PH: 573-308-3538

Prepared By:

QSI Corvallis
1100 NE Circle Blvd, Ste. 126
Corvallis, OR 97330
PH: 541-752-1204

Table of Contents

Table of Contents 2
Introduction 1
Deliverable Products 3
Acquisition 5
Planning 5
Turbidity Measurements 8
Airborne Survey 11
Lidar 11
Digital Imagery 13
Ground Survey 14
Base Stations 14
Ground Survey Points (GSPs) 15
Aerial Targets 16
Land Cover Class 16
Processing 19
Topobathymetric Lidar Data and Sonar Integration 19
Bathymetric Refraction 22
Topobathymetric DEMs 23
Feature Extraction 24
Hydroflattening and Water's Edge Breaklines 24
Contours 25
Digital Imagery 26
Results & Discussion 27
Bathymetric Lidar 27
Mapped Bathymetry and Integrated Coverage 27
Lidar Point Density 30
First Return Point Density 30
Bathymetric and Ground Classified Point Densities 30
Lidar Accuracy Assessments 34
Lidar Non-Vegetated Vertical Accuracy 34
Lidar Vegetated Vertical Accuracies 37
Lidar Bathymetric Vertical Accuracies 38

Lidar Relative Vertical Accuracy 40
Digital Imagery Accuracy Assessment 41
CERTIFICATIONS 46
SELECTED IMAGES 47
GLOSSARY 49
APPENDIX A - ACCURACY CONTROLS 50
APPENDIX B - GMA LIDAR AND SONAR REPORT 51

Cover Photo: A view of the Klamath River near Stanshaw Creek in California. The image is composed of the gridded topobathymetric model and above ground lidar point cloud colored by elevation.

INTRODUCTION



This photo taken by QSI acquisition staff shows a view of the Klamath River just north of the Salmon River confluence.

In June 2018, Quantum Spatial (QSI) was contracted by the United States Geological Survey (USGS), to collect topobathymetric lidar data and digital imagery in the early summer of 2018 for the Klamath River in California and Oregon (contract no. G16PC00016, task order 140G0218F0247). The Klamath River project encompasses the Klamath River corridor AOI, an area of interconnected reservoirs known as Klamath Reservoirs AOI, and several Klamath River tributaries across south central Oregon and northern California. Conventional near-infrared (NIR) lidar was fully integrated with green wavelength (bathymetric) lidar and sonar depth measurements in order to provide a seamless topobathymetric surface dataset. With authorization from the Klamath River Renewal Corporation (KRRC), multibeam and sweep sonar survey data collected by GMA Hydrology, Inc. (GMA), under contract with AECOM Technical Services, Inc. (AECOM), were provided to QSI for the Klamath Reservoirs AOI. Sonar depth measurements taken within the Klamath Reservoirs AOI were incorporated into the lidar dataset to supplement bathymetric bottom returns in areas too deep for lidar mapping. Data were collected to aid USGS in assessing the channel morphology and topobathymetric surface of the study area as part of a comprehensive characterization of the Klamath River prior to dam removal.

This report accompanies the delivered integrated topobathymetric data and imagery, and documents contract specifications, data acquisition procedures, processing methods, sonar integration, and analysis of the final dataset including lidar accuracy, depth penetration, and density. Acquisition dates and acreage are shown in Table 1, a complete list of contracted deliverables provided to USGS is shown in Table 2, and the project extent is shown in Figure 1. Detailed information specific to sonar acquisition, processing, and analysis may be found in the GMA *2018 Klamath Dam Removal Project: Topobathymetric LiDAR & Sonar Technical Data Report,* included as Appendix B.

Table 1: Acquisition dates, acreage, and data types collected on the Klamath River project area

Project Site	Contracted Acres	Buffered Acres	Acquisition Dates	Data Type
Klamath Reservoirs AOI	23,620	26,732	06/11/2018 – 6/13/2018	Topobathymetric lidar
			6/8/2018	4 band (RGB-NIR) Digital Imagery
***Klamath Reservoirs AOI**	8.15	N/A	2/8/2018 – 8/8/2018 5/9/2018 – 5/10/2018 5/29/2018 – 5/30/2018	Multibeam Sonar Sweep Sonar
Klamath River Corridor AOI	40,908	46,004	6/1/2018 – 6/8/2018 6/10/2018 – 6/14/2018	Topobathymetric lidar
			6/8/2018 – 6/23/2018	4 band (RGB-NIR) Digital Imagery

**Acquired by GMA*



This photo taken by QSI's acquisition team shows an oblique aerial view of the Klamath River and Iron Gate Dam, taken from the helicopter during lidar flights.

Deliverable Products

Table 2: Products delivered to USGS for the Klamath River sites

Klamath River Lidar Products Projection: UTM Zone 10 North Horizontal Datum: NAD83 (2011) Vertical Datum: NAVD88 (GEOID12B) Units: Meters	
Topobathymetric Lidar	
Points	LAS v 1.4 PDRF 6 • All Classified Returns • Unclassified Flightline Swaths LAS v 1.4 PDRF9 • Uncalibrated Flightline Swaths • Waveform data (*.wdp)
Rasters	1.0 Meter ERDAS Imagine Files (*.img) • Hydroflattened Bare Earth Digital Elevation Model (DEM) • Topobathymetric Bare Earth Digital Elevation Model (DEM) Clipped • Topobathymetric Bare Earth Digital Elevation Model (DEM) Unclipped • Highest Hit Digital Surface Model (DSM) • Point Density of All Valid Classes 0.5 Meter GeoTiffs • Green Sensor Intensity Images • NIR Sensor Intensity Images
Vectors	Shapefiles (*.shp) • Site Boundary • Tile Index (500m x 500m) • Hydroflattened Breaklines • Water's Edge/Refraction Breaklines • Bathymetric Coverage ESRI File Geodatabase • Flightline Indices • LiDAR Flightline Swath Polygons • Contours (30 cm) Ground Survey Shapefiles (*.shp) • Non-Vegetated Ground Check Points • Vegetated Ground Check Points • Ground Control Points • Ground Control Base Station Coordinates • Bathymetric Check Points • Wetted Edge Check Points • Aerial Targets
4 Band (RGB-NIR) Digital Imagery	
Digital Imagery	15 cm GeoTiffs • Imagery Mosaics (RGB-NIR)

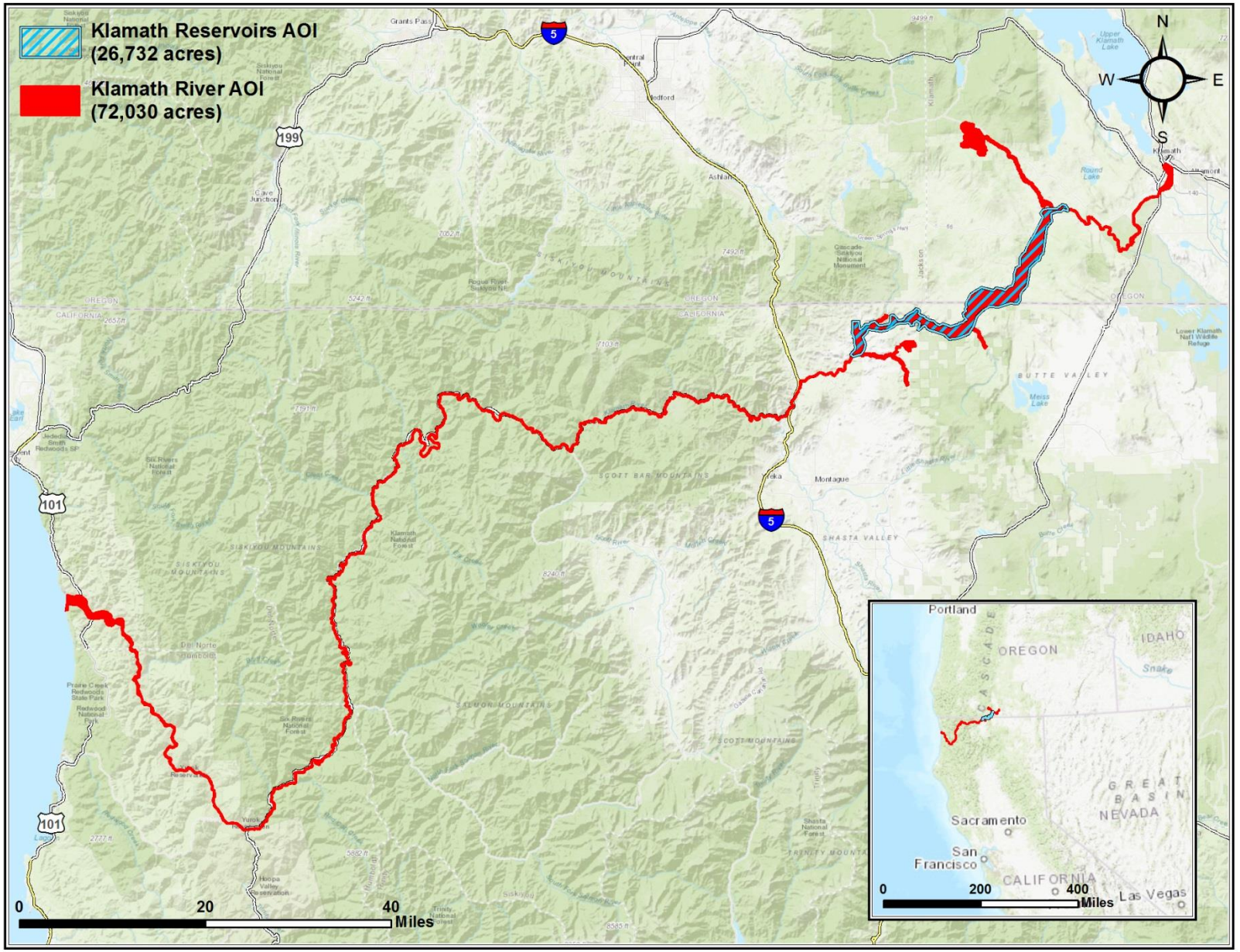


Figure 1: Location map of the Klamath River site in California and Oregon



QSI's Bell 206L-3 Rotorcraft

Planning

In preparation for data collection, QSI reviewed the project area and developed a specialized flight plan to ensure complete coverage of the Klamath River lidar study area at the target combined point density of ≥8 points/m^2 for topographic lidar and ≥2 pulses/m^2 for submerged topobathymetric lidar. Acquisition parameters including orientation relative to terrain, flight altitude, pulse rate, scan angle, and ground speed were adapted to optimize flight paths and flight times while meeting all contract specifications. QSI's Bell 206L-3 Rotorcraft helicopter was selected for acquisition, allowing for a lower flight AGL and increased maneuverability to navigate the narrow Klamath River corridor which passes through the steep terrain of the Pacific Coast Ranges. Due to the lower flight AGL and slower flight speed of the helicopter, LiDAR point density results were expected to be significantly higher than the contracted density requirements.

Factors such as satellite constellation availability and weather windows must be considered during the planning stage. Any weather hazards or conditions affecting the flight were continuously monitored due to their potential impact on the daily success of airborne and ground operations. In addition, logistical considerations including private property access, potential air space restrictions, channel flow rates, and water clarity (Figure 2 and Table 3) were reviewed.

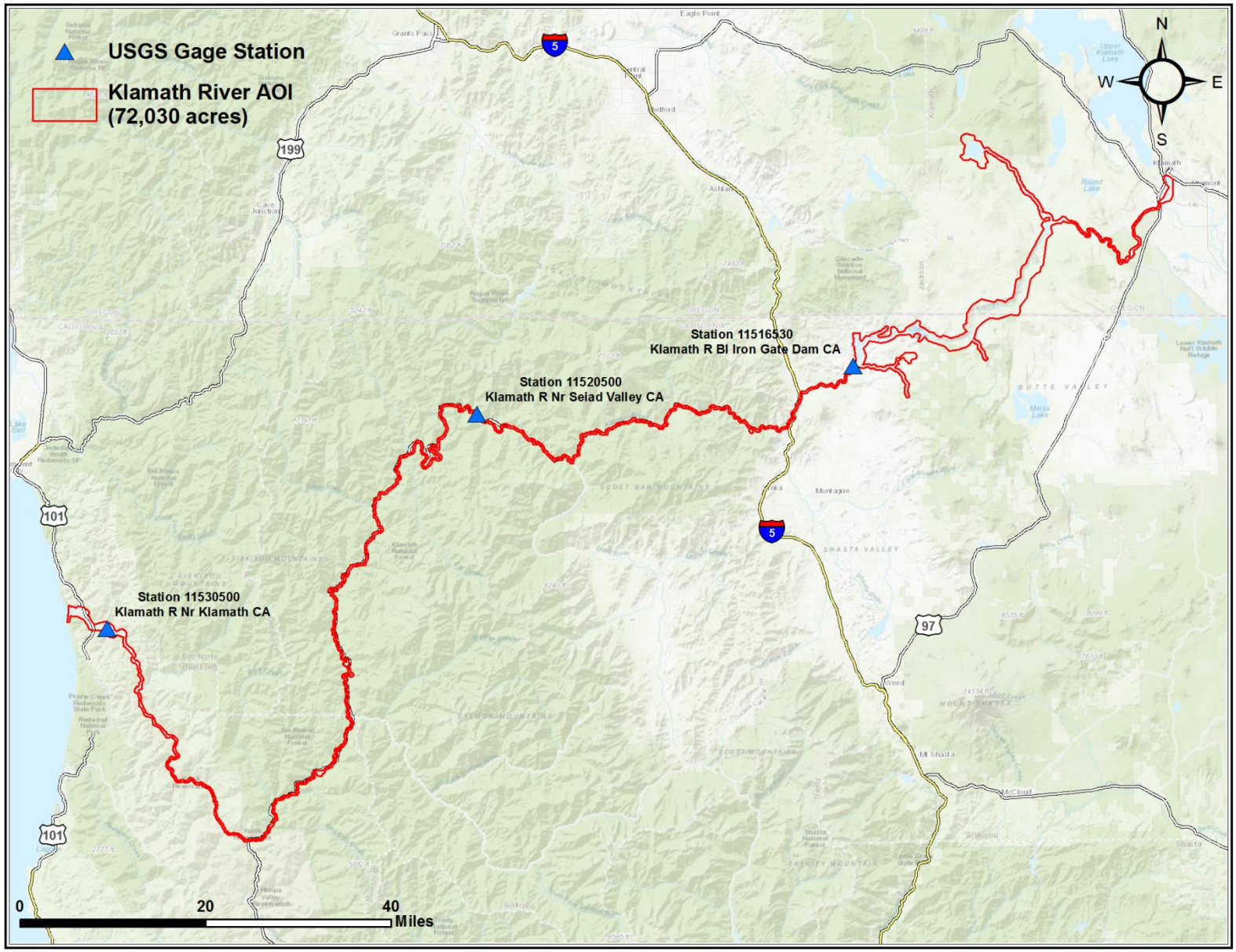


Figure 2: Selected USGS Gage Station locations within the Klamath River site for review of hydrologic conditions at the time of lidar acquisition

Table 3: Hydrologic Conditions for USGS Gage Stations within the Klamath River AOI

USGS Gage Station Daily Average Discharge and Gage Height						
	USGS Gage Station ID					
	11516530		11520500		11530500	
Date	Discharge (cfs)	Gage Height (ft)	Discharge (cfs)	Gage Height (ft)	Discharge (cfs)	Gage Height (ft)
6/1/2018	1111.04	2.28	1917.19	3.06	8606.98	10.58
6/2/2018	1030.42	2.14	1781.56	2.90	8269.38	10.47
6/3/2018	1015.73	2.12	1696.88	2.79	7871.25	10.33
6/4/2018	992.69	2.08	1632.53	2.71	7529.79	10.22
6/5/2018	1004.69	2.10	1607.71	2.68	7271.60	10.13
6/6/2018	1010.10	2.10	1568.65	2.63	7023.02	10.04
6/7/2018	1227.81	2.47	1533.33	2.58	6900.83	10.00
6/8/2018	1590.42	3.04	1852.81	2.98	6923.96	10.01
6/9/2018	1671.25	3.16	2223.23	3.39	7235.21	10.12
6/10/2018	1547.29	2.98	2148.02	3.32	7685.31	10.27
6/11/2018	1419.90	2.79	1993.23	3.14	7413.23	10.18
6/12/2018	1298.13	2.60	1859.58	2.99	6905.52	10.00
6/13/2018	1228.13	2.49	1712.19	2.81	6468.85	9.84
6/14/2018	1164.38	2.38	1645.47	2.73	6123.96	9.72

Turbidity Measurements

In order to assess water clarity conditions prior to and during lidar and digital imagery collection, QSI collected turbidity measurements. Readings were collected at 21 locations throughout the project site between May 31st and June 10th, 2018 Hach 2100Q Turbidimeter. Each day the Hach sensor is calibrated using 4 precise, pre-mixed calibration standards at 10 NTU, 20 NTU, 100 NTU, and 800 NTU. Turbidity observations were recorded three times to confirm measurements. The table below provides turbidity results per location in the Klamath River site.



Figure 3: Hach 2100Q Turbidimeter

Table 4: Turbidity Observations

Turbidity Measurements					
Date	**Latitude**	**Longitude**	**Turbidity Read 1**	**Turbidity Read 2**	**Turbidity Read 3**
31-May	42.218572	-121.787999	5.49	4.97	5.09
1-Jun	42.218725	-121.788300	5.48	4.55	4.77
1-Jun	42.147049	-121.848249	3.67	3.78	3.5
2-Jun	42.135886	-121.942486	6.68	6.42	6.55
2-Jun	42.156311	-122.027328	1.47	1.46	1.49
2-Jun	42.194784	-122.074742	1.34	1.57	1.94
3-Jun	41.899321	-122.508062	3.69	3.02	3.21
3-Jun	41.930857	-122.442271	3.46	3.02	3.54
4-Jun	41.858400	-122.750262	3.03	2.97	2.76
4-Jun	41.823159	-122.961854	2.71	2.71	2.54

4-Jun	41.778788	-123.036589	2.21	2.56	2.01
5-Jun	41.860133	-123.307115	2.35	2.37	2.06
5-Jun	41.789664	-123.379247	1.06	1.01	1.88
5-Jun	41.669281	-123.435820	2.03	1.99	1.64
6-Jun	41.613580	-123.495575	1.91	1.97	2.03
6-Jun	41.377069	-123.493623	1.29	1.52	1.23
7-Jun	41.251671	-123.634851	1.46	1.07	1.01
7-Jun	41.187766	-123.712692	0.95	0.96	0.94
7-Jun	41.342870	-123.856264	0.74	0.95	0.85
8-Jun	41.515948	-124.000319	1.46	1.98	1.39
10-Jun	41.545343	-124.070593	2.79	2.51	2.75



These photos taken by QSI acquisition staff display water clarity conditions in the Klamath River during the time of lidar acquisition. The photo above was taken in the Klamath River shallows near Weitchpec, California and the bottom photo was taken near Midland, Oregon in the Klamath River.



Airborne Survey

Lidar

The lidar survey was accomplished using a Riegl VQ-880-G green laser system mounted in a Bell 206L-3 Rotorcraft. The Riegl VQ-880-G uses a green wavelength (ʎ=532 nm) laser that is capable of collecting high resolution vegetation and topography data, as well as penetrating the water surface with minimal spectral absorption by water. The Riegl VQ-880-G contains an integrated NIR laser (ʎ=1064 nm) that adds additional topography data and aids in water surface modeling. The recorded waveform enables range measurements for all discernible targets for a given pulse. The typical number of returns digitized from a single pulse range from 1 to 7 for the Klamath River project area. It is not uncommon for some types of surfaces (e.g., dense vegetation or water) to return fewer pulses to the lidar sensor than the laser originally emitted. The discrepancy between first return and overall delivered density will vary depending on terrain, land cover, and the prevalence of water bodies. All discernible laser returns were processed for the output dataset. Table 5 summarizes the settings used to yield an average pulse density of ≥8 pulses/m^2 for topographic lidar and ≥2 pulses/m^2 for submerged topobathymetric lidar over the Klamath River project area.

Table 5: Lidar specifications and survey settings

Lidar Survey Settings & Specifications		
Acquisition Dates	June 1 - 8, 2018 June 10 - 14, 2018	
Aircraft Used	Bell 206L-3 Rotorcraft	
Sensor	Riegl	
Laser	VQ-880-G	VQ-880-G-IR
Maximum Returns	15	15
Resolution/Density (Topographic)	Average 8 pulses/m^2	Average 8 pulses/m^2
Resolution/Density (Submerged)	Average 2 pulses/m^2	n/a
Nominal Pulse Spacing	0.7 m	0.35 m
Survey Altitude (AGL)	400 m	400 m
Survey speed	60 knots	60 knots
Field of View	40°	40°
Mirror Scan Rate	80 lines per second	Uniform point spacing
Target Pulse Rate	245 kHz	245 kHz
Pulse Length	1.5 ns	3 ns
Laser Pulse Footprint Diameter	28 cm	8 cm
Central Wavelength	532 nm	1064 nm
Pulse Mode	Multiple Times Around (MTA)	Multiple Times Around (MTA)
Beam Divergence	0.7 mrad	0.2 mrad
Swath Width	291 m	291 m
Swath Overlap	30 %	30 %
Intensity	16-bit	16-bit
Accuracy	$RMSE_Z \leq 18.5$ cm	$RMSE_Z \leq 18.5$ cm

To accurately solve for laser point position (geographic coordinates x, y and z), the positional coordinates of the airborne sensor and the attitude of the aircraft were recorded continuously throughout the lidar data collection mission. Position of the aircraft was measured twice per second (2 Hz) by an onboard differential GPS unit, and aircraft attitude was measured 200 times per second (200 Hz) as pitch, roll and yaw (heading) from an onboard inertial measurement unit (IMU). To allow for post-processing correction and calibration, aircraft and sensor position and attitude data are indexed by GPS time.



Another photo taken by QSI's acquisition team shows an oblique aerial view of the mouth of the Klamath River at the Pacific Ocean, taken from the helicopter during lidar flights.

Digital Imagery

Aerial imagery was collected using an UltraCam XP and an UltraCam Falcon digital mapping camera (Table 6). The systems were gyro-stabilized and simultaneously collected panchromatic and multispectral (RGB, NIR) imagery.

Table 6: Camera manufacturer's specifications

UltraCam XP/Falcon Specifications	
Focal Length	100.5 mm
Data Format	RGB, NIR
RCD Pixel Size	6.0 µm
Image Size	17,310 x 11,310 pixels
Frame Rate	2.0 sec (GPS triggered)
FOV	55 x 37 deg

For the Klamath River Topobathy project, 1,781 images were collected with 60% along track overlap and 40% sidelap between frames. The acquisition flight parameters were designed to yield a native pixel resolution of ≤ 15 cm. Orthophoto specifications particular to the Klamath River survey are shown in Table 7.

Table 7: Project-specific orthophoto specifications

Digital Orthophotography Specifications	
Equipment	UltraCam XP/Falcon
Spectral Bands	Red, Green, Blue, NIR
Ground Sampling Distance	≤ 15 cm
Along Track Overlap	≥60%
Cross Track Overlap	≥40%
Flight Altitude (AGL)	2,500 meters
Data Format	8-bit GeoTiff

Ground Survey

Ground control surveys, including base stations, aerial targets and ground survey points (GSPs), were conducted by QSI to support the airborne acquisition. Ground control data were used to geospatially correct the aircraft positional coordinate data and to perform quality assurance checks on final lidar data and orthoimagery products.



QSI-Established Base

Base Stations

Base stations supported collection of ground survey points using real time kinematic (RTK), post processed kinematic (PPK), and fast static (FS) survey techniques. Base station locations were selected with consideration for satellite visibility, field crew safety, and optimal location for GSP coverage. QSI utilized four NGS monuments, two Leica SmartNet Real Time Network (RTN) base stations, two Oregon Real-time GNSS Network (ORGN) RTN base stations, and four newly-established monuments for the Klamath River lidar project (Table 8, Figure 4). New base stations were set using 5/8" x 30" rebar topped with stamped 2 ½ " aluminum caps. QSI's professional land surveyor, Evon P. Silvia (ORPLS#81104, CAPLS#9401) oversaw and certified the establishment of all base stations.

Table 8: Base Stations utilized for the Klamath River acquisition. Coordinates are on the NAD83 (2011) datum, epoch 2010.00

Base Station ID	Latitude	Longitude	Ellipsoid (meters)	Base Station Type
AF8313	41° 49' 30.52025"	-122° 58' 24.29385"	473.696	NGS Monument
AF8314	41° 51' 50.48136"	-122° 43' 43.47429"	544.379	NGS Monument
DH6358	41° 21' 03.63961"	-123° 30' 09.86520"	186.278	NGS Monument
DH6353	41° 14' 25.69661"	-123° 39' 20.34297"	99.125	NGS Monument
KLAM_RTK_01	41° 55' 53.60915"	-122° 26' 30.05496"	644.842	QSI Monument
KLAM_RTK_02	41° 39' 41.28374"	-123° 26' 59.92257"	254.391	QSI Monument
KLAM_RTK_03	41° 16' 43.30246"	-123° 49' 58.88685"	75.561	QSI Monument
KLAM_RTK_04	41° 30' 34.28502"	-123° 59' 24.17923"	-15.150	QSI Monument
ORKF	42° 08' 36.16180"	-121° 48' 31.06952"	1235.036	Leica SmartNet RTN
P380	42° 15' 34.79886"	-121° 46' 46.85526"	1391.280	ORGN RTN
P784	41° 49' 50.92289"	-122° 25' 13.58557"	802.702	ORGN RTN
P154	41° 48' 25.48411"	-123° 21' 36.12405"	320.323	Leica SmartNet RTN

To correct the continuously recorded onboard measurements of the aircraft position, QSI concurrently conducted multiple static Global Navigation Satellite System (GNSS) ground surveys (1 Hz recording frequency) over each base station. During post-processing, the static GPS data were triangulated with nearby Continuously Operating Reference Stations (CORS) using the Online Positioning User Service

(OPUS[1]) for precise positioning. Multiple independent sessions over the same base station were processed to confirm antenna height measurements and to refine position accuracy.

Ground Survey Points (GSPs)

Ground survey points were collected using RTK, PPK, and FS survey techniques. For an RTK survey, a roving receiver receives corrections from a nearby base station or Real-Time Network (RTN) via radio or cellular network, enabling rapid collection of points with relative errors less than 1.5 cm horizontal and 2.0 cm vertical. PPK and FS surveys compute these corrections during post-processing to achieve comparable accuracy. RTK and PPK surveys record data while stationary for at least five seconds, calculating the position using at least three one-second epochs. FS surveys record observations for up to fifteen minutes on each GSP in order to support longer baselines for post-processing. All GSP measurements were made during periods with a Position Dilution of Precision (PDOP) of ≤ 3.0 with at least six satellites in view of the stationary and roving receivers. See Table 9 for QSI ground survey equipment specifications.

GSPs were collected in areas where good satellite visibility was achieved on paved roads and other hard surfaces such as gravel or packed dirt roads. GSP measurements were not taken on highly reflective surfaces such as center line stripes or lane markings on roads due to the increased noise seen in the laser returns over these surfaces. GSPs were collected within as many flightlines as possible; however, the distribution of GSPs depended on ground access constraints and base station locations and may not be equitably distributed throughout the study area (Figure 4).

Table 9: Trimble equipment identification

Receiver Model	Antenna	OPUS Antenna ID	Use
Trimble R7 GNSS	Zephyr GNSS Geodetic Model 2 RoHS	TRM57971.00	Static
Trimble R8	Integrated Antenna R8 Model 2	TRM_R8_GNSS	Rover

[1] OPUS is a free service provided by the National Geodetic Survey to process corrected base station positions. http://www.ngs.noaa.gov/OPUS/.

Aerial Targets

Aerial targets were identified throughout the project area prior to imagery acquisition in order to geo-spatially correct the orthoimagery (Figure 4). Air targets used for the Klamath River project consisted of spray-painted chevrons and existing permanent photo-identifiable features painted on asphalt such as handicap parking signs, stop bars, and turn lane arrows. Each target was precisely located using one FS point.



Land Cover Class

In addition to ground survey points, land cover class check points were collected throughout the study area to evaluate vertical accuracy. Vertical accuracy statistics were calculated for all land cover types to assess confidence in the lidar derived ground models across land cover classes (Table 10, see Lidar Accuracy Assessments).

Table 10: Land Cover Types and Descriptions

Land cover type	Land cover code	Example	Description	Accuracy Assessment Type
Shrubland	SHRUB		Maintained or low growth herbaceous grasslands	VVA
Tall Grass	TALL_GRASS		Herbaceous grasslands in advanced stages of growth	VVA
Bare Earth	BARE, BE		Areas of bare earth surface	NVA
Urban	URBAN		Areas dominated by urban development, including parks	NVA

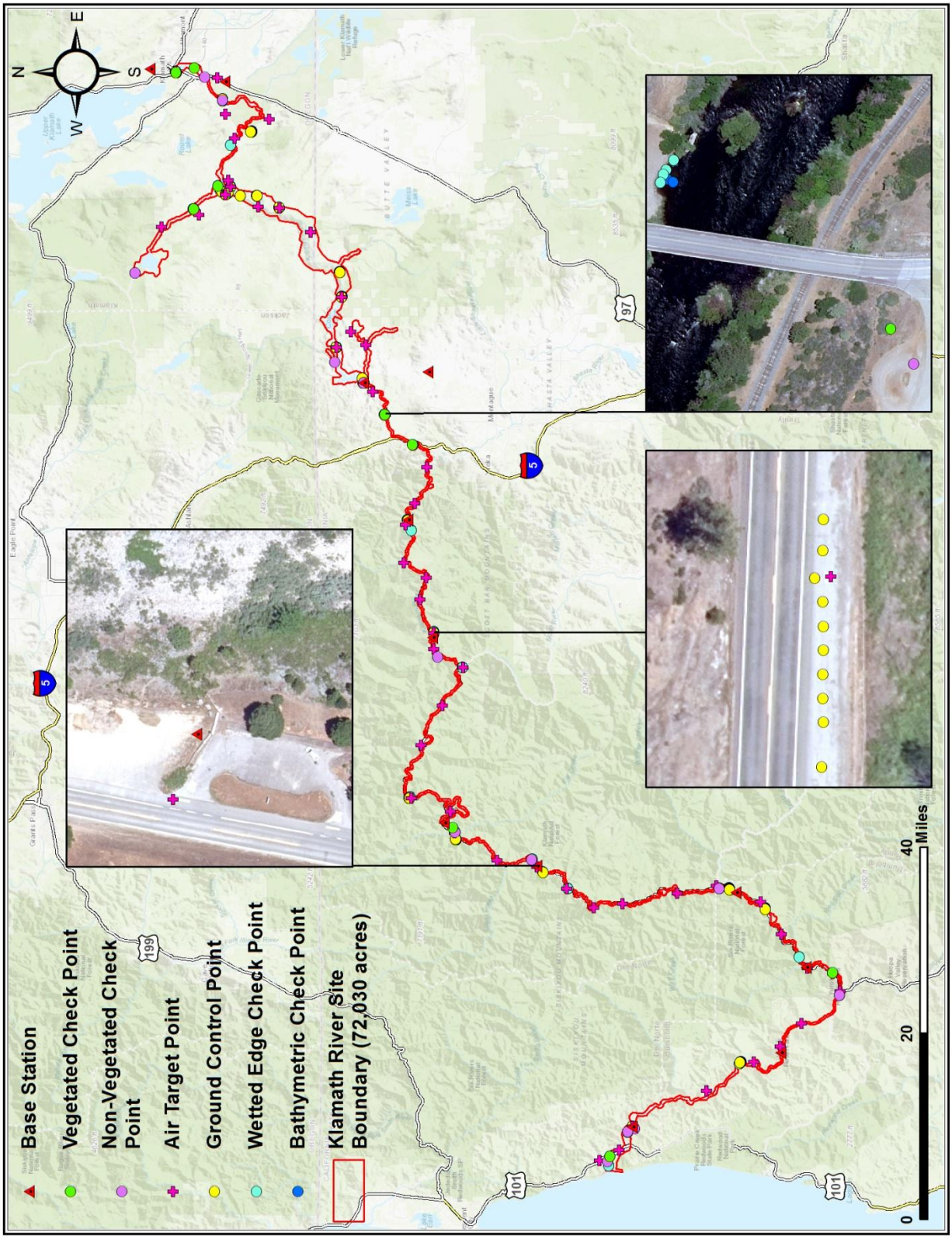
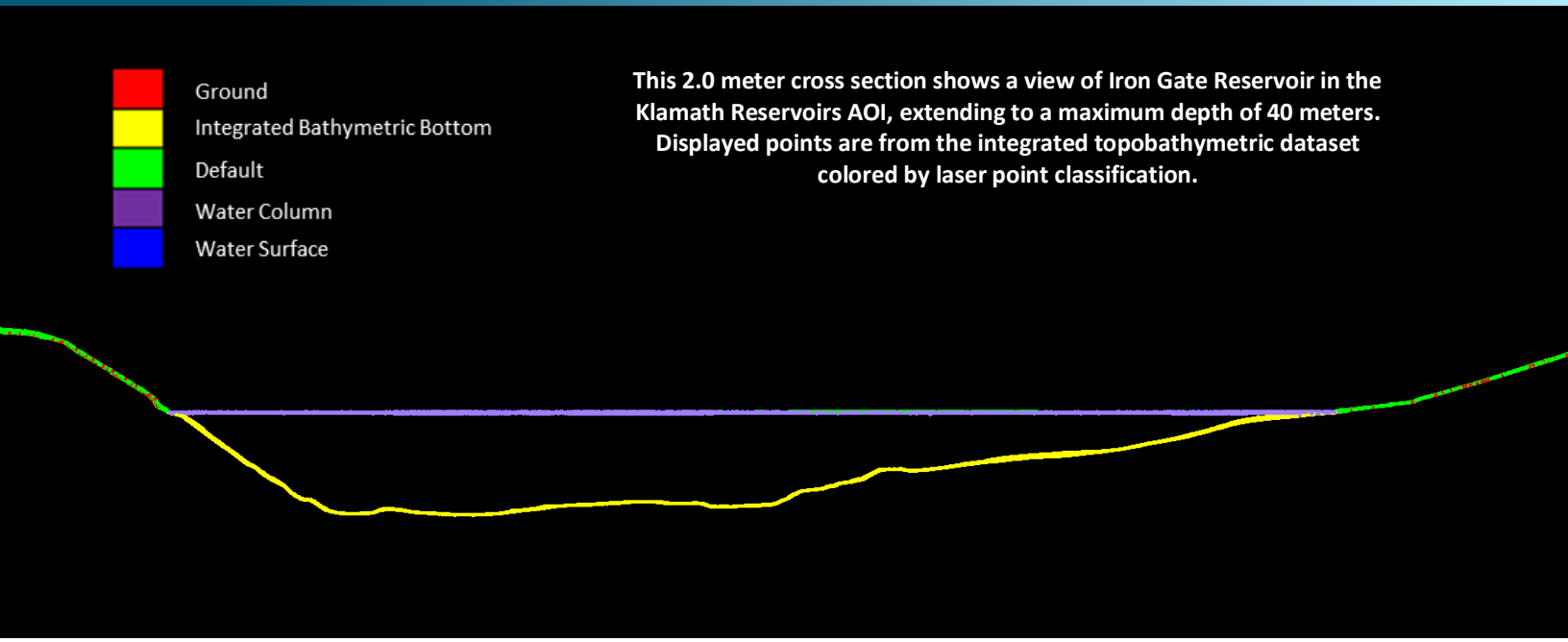


Figure 4: Ground survey location map



This 2.0 meter cross section shows a view of Iron Gate Reservoir in the Klamath Reservoirs AOI, extending to a maximum depth of 40 meters. Displayed points are from the integrated topobathymetric dataset colored by laser point classification.

Topobathymetric Lidar Data and Sonar Integration

Upon completion of data acquisition, QSI processing staff initiated a suite of automated and manual techniques to process the data into the requested deliverables. Processing tasks included GPS control computations, smoothed best estimate trajectory (SBET) calculations, kinematic corrections, calculation of laser point position, sensor and data calibration for optimal relative and absolute accuracy, and lidar point classification (Table 11).

Riegl's RiProcess software was used to facilitate bathymetric return processing. Once bathymetric points were differentiated, they were spatially corrected for refraction through the water column based on the angle of incidence of the laser. QSI refracted water column points using QSI's proprietary LAS processing software, Las Monkey. The resulting point cloud data were classified using both manual and automated techniques.

GMA performed all multibeam and sweep sonar data acquisitions and used Caris HIPS v. 10 to process and edit raw track lines to remove any noise and to evaluate the data for visual anomalies. Sonar data was provided to QSI in LAS 1.4 format. QSI imported the multibeam and sweep sonar, as Class 40 (Bathymetric Bottom), into the existing topobathymetric lidar dataset using Bentley Microstation and Terrasolid software. Processing methodologies were tailored for the landscape. Brief descriptions of these tasks are shown in Table 12.

Table 11: ASPRS LAS classification standards applied to the Klamath River dataset

Classification Number	Classification Name	Classification Description
1	Default/Unclassified	Laser returns that are not included in the ground class, composed of vegetation and anthropogenic features
1-O	Default/Unclassified Overlap	Flightline edge clip that is withheld because it does not contribute to the utility of the dataset, but may be maintained as a reference
2	Ground	Laser returns that are determined to be ground using automated and manual cleaning algorithms
3	Low Vegetation	Laser returns between 0.25 and 2 meters that were classified as vegetation using an automated routine
4	Medium Vegetation	Laser returns between 2 and 5 meters that were classified as vegetation using an automated routine
5	High Vegetation	Laser returns above 5 meters that were classified as vegetation using an automated routine
7	Noise	Laser returns that are often associated with birds, scattering from reflective surfaces, or artificial points below the ground surface
9	NIR Water Surface	NIR laser returns that are determined to be water using automated and manual cleaning algorithms
17	Bridge	Bridge decks
20	Ignored Ground	Ground points proximate to water's edge breaklines; ignored for correct model creation
22	Temporal Exclusion	Non-favored data in intertidal zones
40	Lidar Bathymetric Bottom	Refracted Riegl sensor returns that fall within the water's edge breakline which characterize the submerged topography and integrated sonar data
41	Green Water Surface	Green laser returns that are determined to be water surface points using automated and manual cleaning algorithms
45	Water Column	Refracted Riegl sensor returns that are determined to be water using automated and manual cleaning algorithms
80	Sonar Bathymetric Bottom	Binned sonar returns that were collected with a multi-transducer sonar sweep system
81	Sonar Bathymetric Bottom	Binned sonar returns that were collected with a multibeam sonar system

Table 12: Lidar and sonar integration processing workflow

Lidar Processing Step	Software Used	Processor
Resolve kinematic corrections for aircraft position data using kinematic aircraft GPS and static ground GPS data. Develop a smoothed best estimate of trajectory (SBET) file that blends post-processed aircraft position with sensor head position and attitude recorded throughout the survey.	POSPac MMS v.8.2	QSI
Calculate laser point position by associating SBET position to each laser point return time, scan angle, intensity, etc. Create raw laser point cloud data for the entire survey in *.las (ASPRS v. 1.4) format. Convert data to orthometric elevations by applying a geoid correction.	RiProcess v1.8.5 TerraMatch v.18	QSI
Import raw laser points into manageable blocks (less than 500 MB) to perform manual relative accuracy calibration and filter erroneous points. Classify ground points for individual flight lines.	TerraScan v.18	QSI
Using ground classified points per each flight line, test the relative accuracy. Perform automated line-to-line calibrations for system attitude parameters (pitch, roll, heading), mirror flex (scale) and GPS/IMU drift. Calculate calibrations on ground classified points from paired flight lines and apply results to all points in a flight line. Use every flight line for relative accuracy calibration.	TerraMatch v.18 RiProcess v.1.8.2	QSI
Apply refraction correction to all subsurface returns.	Las Monkey 2.3 (QSI proprietary software)	QSI
*Collect multibeam and sweep sonar. Process and edit raw track lines to remove any noise. Evaluate data for visual anomalies and perform quality assurance checks.	Caris HIPS v. 10	GMA
Import multibeam Sonar data into LiDAR point cloud	TerraScan v.18 TerraModeler v.18	QSI
Classify resulting data to ground and other client designated ASPRS classifications (Table 11). Assess statistical absolute accuracy via direct comparisons of ground classified points to ground control survey data.	TerraScan v.18 TerraModeler v.18	QSI
Generate bare earth models as triangulated surfaces. Generate highest hit models as a surface expression of all classified points. Export all surface models in ERDAS Imagine (.img) format 1 meter pixel resolution.	Las Product Creator 3.0 (QSI proprietary software)	QSI
Export intensity images as GeoTIFFs at a 0.5 meter pixel resolution.	Las Product Creator 3.0 (QSI proprietary software)	QSI

**See Appendix B for detailed explanation of sonar processing*

Bathymetric Refraction

Green lidar pulses that enter the water column must have their position corrected for refraction of the light beam as it passes through the water and its resulting decreased speed. QSI has developed proprietary software (Las Monkey) to perform this processing based on Snell's law. The first step is to develop a water surface model (WSM) from the NIR lidar water surface returns.

Depending on the degree of water level fluctuation due to temporal changes in water elevation, QSI implemented two different methods to generate WSMs. For water bodies considered "calm" with relatively static water levels, the WSM used for refraction is generated using NIR points within the breaklines defining the water's edge. Points are filtered and edited to obtain the most accurate representation of the water surface and are used to create a water surface model TIN.

For water bodies exposed to tidal or wave action, the method of WSM generation factors in significant temporal changes in water surface elevation over the time of acquisition. NIR lidar returns are used to determine the water surface level and water surface points are classified for both forward and reverse look directions of the green scanner. The points are filtered and edited to obtain the most accurate representation of the water surface and are used to generate a WSM for each flight line and look direction. Each look direction (forward and reverse) are modeled separately to correctly model short duration time dependent surface changes (e.g. waves) that change between the times that each look direction records a unique location. The WSM created is raster based with an associated surface normal vector to obtain the most accurate angle of incidence during refraction.

Once all WSMs are generated, the Las Monkey refraction software then intersects the partially submerged green pulses with the WSM to determine the angle of incidence with the water surface and the submerged component of the pulse vector. This provides the information necessary to correct the position of underwater points by adjusting the submerged vector length and orientation. After refraction, the points are compared against bathymetric check points to assess accuracy.

Both methods of WSM generation were implemented for the Klamath River AOI project. At the Klamath River mouth, where the river empties into the Pacific Ocean, the method incorporating tidal and wave action was used to generate the WSM. All other areas of the Klamath River AOI were refracted using a WSM that assumed water levels remained relatively static during acquisition.

Topobathymetric DEMs

Bathymetric bottom lidar returns can be limited by depth, water clarity, and bottom surface reflectivity. Water clarity and turbidity affect the depth penetration capability of the green wavelength lidar with returning laser energy diminishing by scattering throughout the water column. Additionally, the bottom surface must be reflective enough to return remaining laser energy back to the sensor at a detectable level. Likewise, the multibeam and sweep sonar collection is limited by obstructions within the river channel and proximity to the shoreline, due to safety procedures for crew and equipment. Therefore, it is not unexpected to have no bathymetric bottom returns in turbid, non-reflective, or obstructed areas.

As a result, creating digital elevation models (DEMs) presents a challenge with respect to interpolation of areas with no returns. Traditional DEMs are "unclipped", meaning areas lacking ground returns are interpolated from neighboring ground returns (or breaklines in the case of hydro-flattening), with the assumption that the interpolation is close to reality. In bathymetric modeling, these assumptions are prone to error because a lack of bathymetric returns can indicate a change in elevation that the sensors can no longer map due to increased or decreased depths. The resulting void areas may suggest varying depths, rather than similar elevations from neighboring bathymetric bottom returns. Therefore, QSI created a final water polygon with bathymetric coverage to delineate areas with successfully mapped bathymetry from lidar and sonar integration. This shapefile was used to clip the extent of the final integrated topobathymetric model to avoid false triangulation (interpolation from TIN'ing) across areas in the water with no mapped bathymetry.

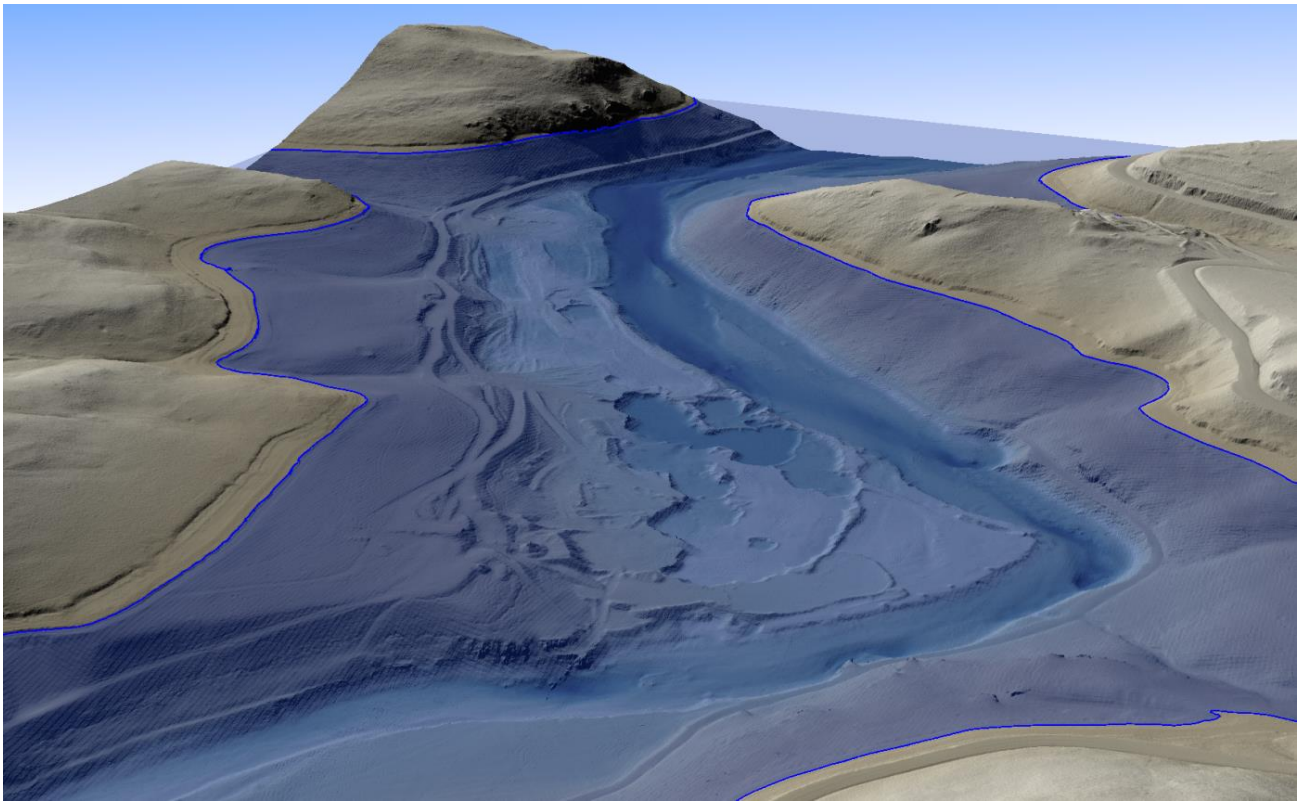


Figure 5: A view looking down at the Iron Gate Reservoir showing bathymetric depths up to 38 meters. This image was created from the integrated topobathymetric bare earth model colored by elevation. A simulated water level is inserted into the image at an elevation of 707 meters.

Feature Extraction

Hydroflattening and Water's Edge Breaklines

The Klamath River and other water bodies within the project area were flattened to a consistent water level. Bodies of water that were flattened include lakes and other closed water bodies with a surface area greater than 2 acres, all streams and rivers that are nominally wider than 30 meters, all tidal waters bordering the project, and select smaller bodies of water as feasible. The hydroflattening process eliminates artifacts in the digital terrain model caused by both increased variability in ranges or dropouts in laser returns due to the low reflectivity of water.

Hydroflattening of closed water bodies was performed through a combination of automated and manual detection and adjustment techniques designed to identify water boundaries and water levels. Boundary polygons were developed using an algorithm which weights lidar-derived slopes, intensities, and return densities to detect the water's edge. The water edges were then manually reviewed and edited as necessary.

Once polygons were developed the initial ground classified points falling within water polygons were reclassified as water points to omit them from the final ground model. Elevations were then obtained from the filtered lidar returns to create the final breaklines. Lakes were assigned a consistent elevation for an entire polygon while rivers were assigned consistent elevations on opposing banks and smoothed to ensure downstream flow through the entire river channel.

Water boundary breaklines were then incorporated into the hydroflattened DEM by enforcing triangle edges (adjacent to the breakline) to the elevation values of the breakline. This implementation corrected interpolation along the hard edge.

Contours

Contour generation from lidar point data required a thinning operation in order to reduce contour sinuosity. The thinning operation reduced point density where topographic change is minimal (i.e., flat surfaces) while preserving resolution where topographic change was present. Model key points were selected from the ground classified points with the spacing decreased in regions with high surface curvature. Generation of model key points eliminated redundant detail in terrain representation, particularly in areas of low relief, and provided for a more manageable dataset. Contours were produced through TerraModeler by interpolating between the model key points at even elevation increments.

Elevation contour lines were then intersected with ground point density raster models and a confidence field was added to each contour line. Contours which crossed areas of high point density have high confidence levels, while contours which crossed areas of low point density have low confidence levels. Areas with low ground point density are commonly beneath buildings and bridges, in locations with dense vegetation, over water, and in other areas where laser penetration to the ground surface was impeded (Figure 6).

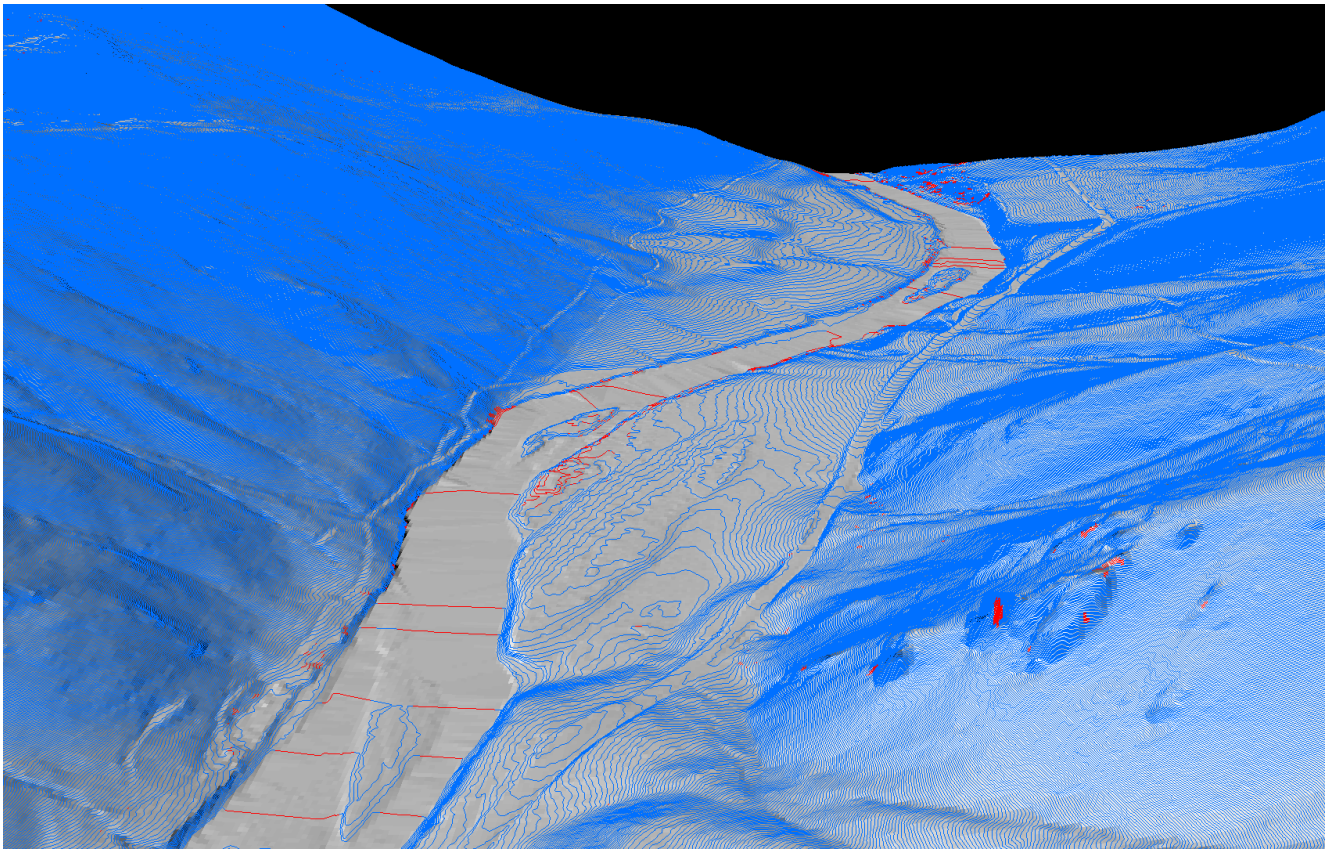


Figure 6: Contours draped over the Klamath River bare earth elevation model located east of Copco Lake. Blue contours represent high confidence while the red contours represent low confidence.

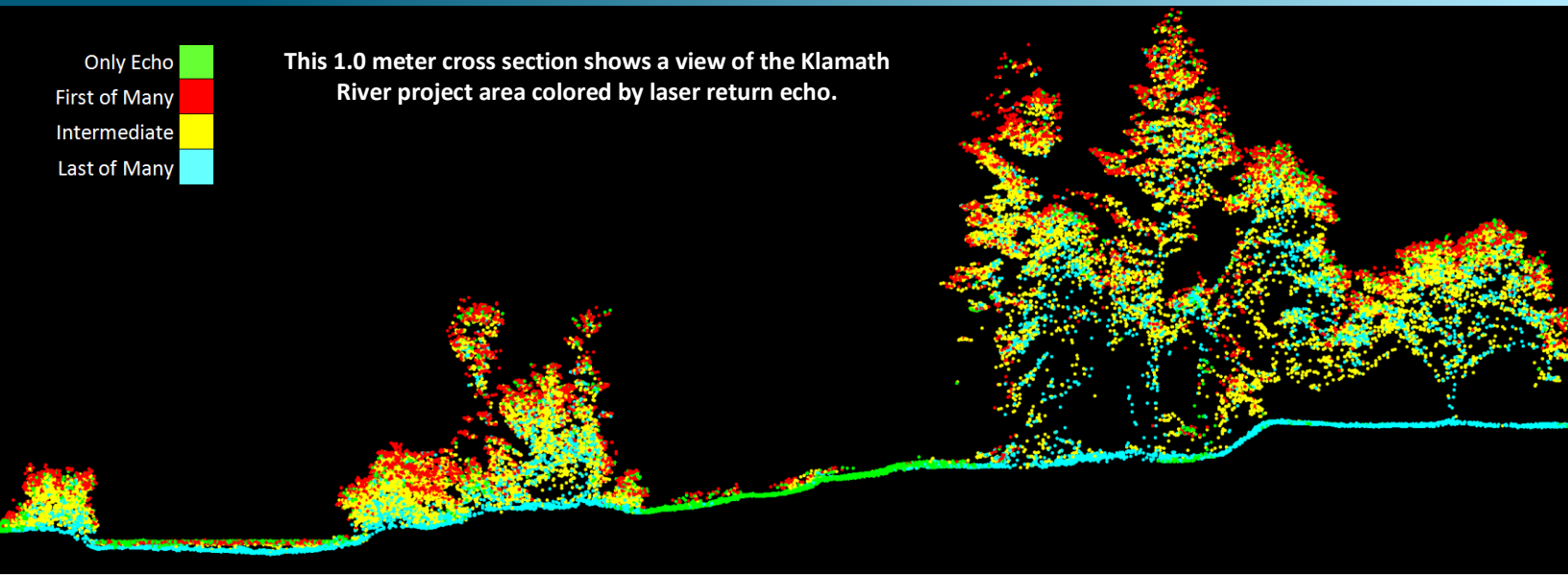
Digital Imagery

The collected digital photographs went through multiple processing steps to create final orthophoto products. Initially, images were corrected for geometric distortion to yield level02 image files. Next, images were color balanced and levels were adjusted to exploit the full 14-bit histogram and finally output as level03 pan-sharpened 8bit TIFF images. Camera position and orientation were calculated by linking the time of image capture to the smoothed best estimate of trajectory (SBET). Within Inpho's Match AT softcopy photogrammetric software, analytical aerial triangulation was performed using ground control, automatically generated tie points, and camera calibration information.

Adjusted images were orthorectified using the lidar-derived ground model to remove displacement effects from topographic relief inherent in the imagery. The resulting orthos were mosaicked within Inpho's OrthoVista blending seams and applying automated project color-balancing. The final mosaics were inspected and edited for seam cutlines across above ground features such as buildings and other man-made features. Special care was taken to eliminate glare on the water surface, in some instances this resulted in introducing tree lean along the river shoreline. The processing workflow for orthophotos is summarized in Table 13.

Table 13: Orthophoto processing workflow

Orthophoto Processing Step	Software Used
Resolve GPS kinematic corrections for the aircraft position data using kinematic aircraft GPS (collected at 2 Hz) and static ground control data.	Inertial Explorer v8.7
Develop a smooth best estimate trajectory (SBET) file that blends post-processed aircraft position with attitude data. Sensor heading, position, and attitude are calculated throughout the survey.	Inertial Explorer v8.7
Create an exterior orientation file (EO) for each photo image with omega, phi, and kappa.	Inertial Explorer v8.7
Convert Level 00 raw imagery data into geometrically corrected Level 02 image files.	UltraMap v4
Apply radiometric adjustments to Level 02 image files to create Level 03 Pan-sharpened TIFFs.	UltraMap v4
Apply EO to photos, measure ground control points and perform aerial triangulation.	Inpho Match AT v8
Use lidar derived DEM to create distortion free ortho images.	Inpho OrthoMaster v8
Mosaic orthorectified imagery, blending seams between individual photos and correcting for radiometric differences between photos.	Inpho OrthoVista/SeamEditor v8



Bathymetric Lidar

An underlying principle for collecting hydrographic lidar data is to survey near-shore areas that can be difficult to collect with other methods, such as sonar. Lidar excels in shallow bathymetric environments, particularly over large areas, but bathymetric detection at greater depths is limited up to the laser depth penetration range. Deep bathymetric environments are more favorable to sonar collection methods due to the sound wave's greater capacity to propagate through water. Sonar data may be used to compliment topobathymetric lidar surveys by providing bathymetric depth measurements in areas exceeding the laser penetration range. Sites like the Klamath River AOI that exhibit shallow and deep bathymetric environments offer an opportunity to integrate sonar with lidar data to create a comprehensive seamless topobathymetric model of the project site.

All available multibeam and sweep sonar data was integrated with the final topobathymetric lidar dataset. In order to assess the overall integrated bathymetric dataset, several parameters were considered; depth penetrations below the water surface, bathymetric return density, and spatial accuracy.

Mapped Bathymetry and Integrated Coverage

QSI reviewed bathymetric coverage and void results for the Klamath River project in lidar-only areas, as well as the fully integrated lidar and sonar dataset. Insufficiently mapped areas were identified by triangulating bathymetric bottom points with an edge length maximum of 4.56 meters. This ensured all areas of no returns (> 9 m^2), were identified as data voids.

In total, approximately 65.65% of the Klamath River and Reservoirs sites were mapped with bathymetric bottom data. Additionally, bathymetric coverage increased from 4,686 acres with lidar only data, to 6,466 acres after sonar integration.

QSI also reviewed the mapped depths of identified coverage areas; in lidar-only areas, 47.37% of bathymetric bottom returns were up to one foot deep. In fully integrated areas, depths of up to 47 meters were mapped. Table 15 and Table 16 below provide depth and coverage information for the lidar-only sites, as well as the full, integrated dataset.

Table 14: Fully integrated lidar and sonar bathymetric bottom coverage results by depth

Depth (m)	Percent of "Covered" Area (%)	Total Area (acres)
< 5	33.50%	659.73
5 - 10	18.85%	371.30
10 -15	14.83%	292.00
15 - 20	12.61%	248.39
20 -25	8.49%	167.16
25 - 30	4.12%	81.22
30 - 35	3.85%	75.73
35 - 40	2.87%	56.55
40 - 45	0.86%	16.86
45 - 47	0.02%	0.47

Table 15: Lidar-only bathymetric bottom coverage results by depth

Depth (m)	Percent of "Covered" Area (%)	Area (acres)
< 0.49	23.57%	1,029.97
0.49 - 1.0	23.80%	1,039.74
1.0 - 1.49	18.82%	822.35
1.5 - 1.99	13.55%	591.97
2.0 - 2.49	9.08%	396.82
2.5 - 2.99	6.12%	267.61
3.0 - 3.49	3.60%	157.09
3.5 - 3.99	1.28%	56.15
4.0 - 4.49	0.17%	7.25
4.5 - 4.99	0.01%	0.34
> 5.0	0.00%	0.04

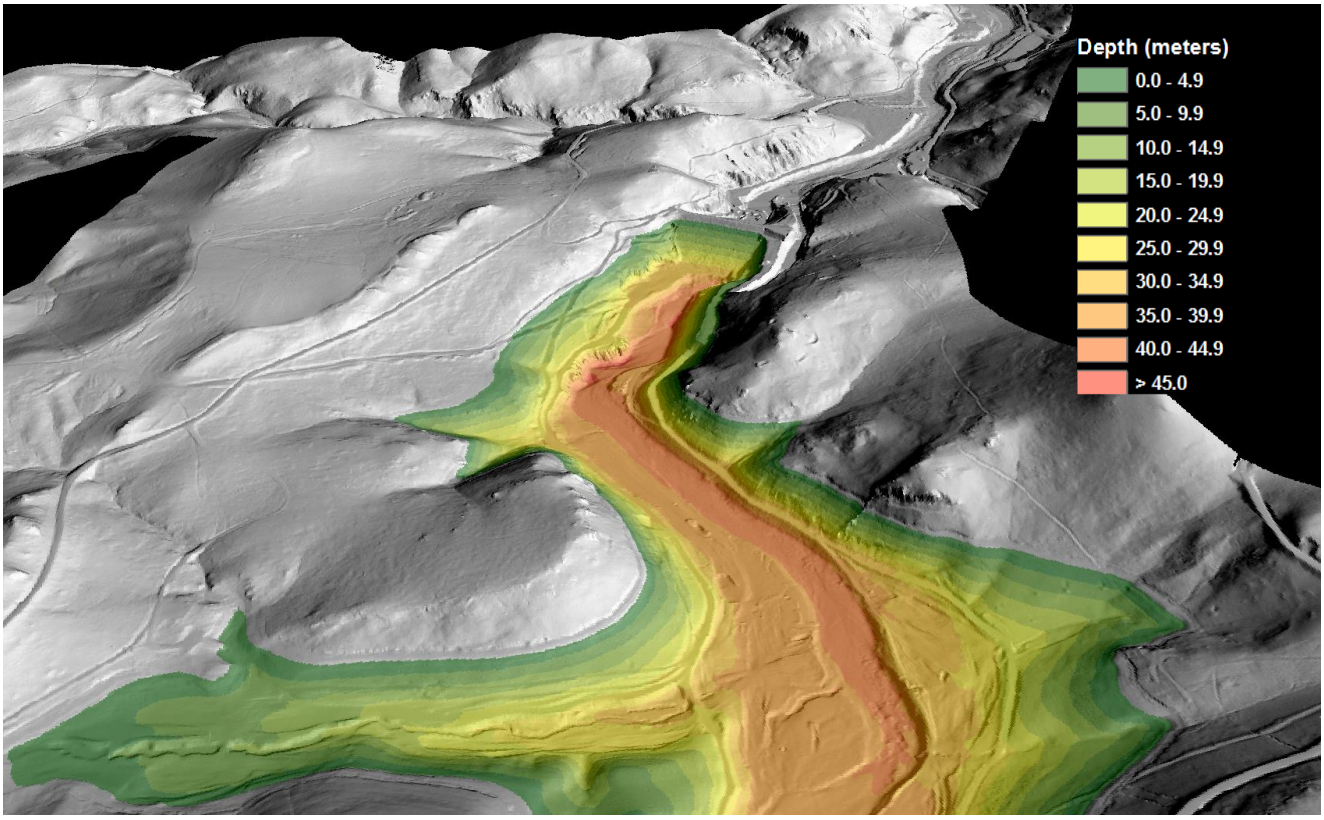


Figure 7: A south facing view looking down at the Iron Gate Reservoir showing bathymetric depths up to 47 meters. This image was created from the integrated topobathymetric bare earth hill shade overlain by a water depth model colored by depth.

Lidar Point Density

First Return Point Density

The acquisition parameters were designed to acquire a minimum first-return density of ≥8 points/m^2. Due to the low AGL and slower flight speed of the helicopter used to acquire lidar data, point density results were anticipated to be much higher than contract requirements.

First return density describes the density of pulses emitted from the laser that return at least one echo to the system. Multiple returns from a single pulse were not considered in first return density analysis. Some types of surfaces (e.g., breaks in terrain, water and steep slopes) may have returned fewer pulses than originally emitted by the laser. First returns typically reflect off the highest feature on the landscape within the footprint of the pulse. In forested or urban areas the highest feature could be a tree, building or power line, while in areas of unobstructed ground, the first return will be the only echo and represents the bare earth surface.

The average first-return density of the Klamath River lidar project was 49.20 points/m^2 (Table 16). The statistical and spatial distributions of all first return densities per 100 m x 100 m cell are portrayed in Figure 8 and Figure 10.

Bathymetric and Ground Classified Point Densities

The density of ground classified lidar and bathymetric bottom returns were also analyzed for this project. Terrain character, land cover, and ground surface reflectivity all influenced the density of ground surface returns. In vegetated areas, fewer pulses may have penetrated the canopy, resulting in lower ground density. Similarly, the density of bathymetric bottom returns was influenced by turbidity, depth, and bottom surface reflectivity. In turbid areas, fewer pulses may have penetrated the water surface, resulting in lower bathymetric density.

The ground and bathymetric bottom classified density of lidar data for the Klamath River project was 5.37 points/m^2 (Table 16). The statistical and spatial distributions ground classified and bathymetric bottom return densities per 100 m x 100 m cell are portrayed in Figure 9 and Figure 11.

Additionally, acquisition parameters for the Klamath River project specified an average bathymetric bottom return density value of ≥2 points/m^2. Bathymetric bottom returns were calculated for areas containing at least one bathymetric bottom return. Areas lacking bathymetric returns were not considered in calculating an average density value. Within the successfully mapped area, a bathymetric bottom return density of 9.18 points/m^2 was achieved.

Table 16: Average lidar point densities

Density Type	Point Density
First Returns	49.20 points/m²
Ground and Bathymetric Bottom Classified Returns	5.37 points/m^2
Bathymetric Bottom Classified Returns	9.18 points/m²

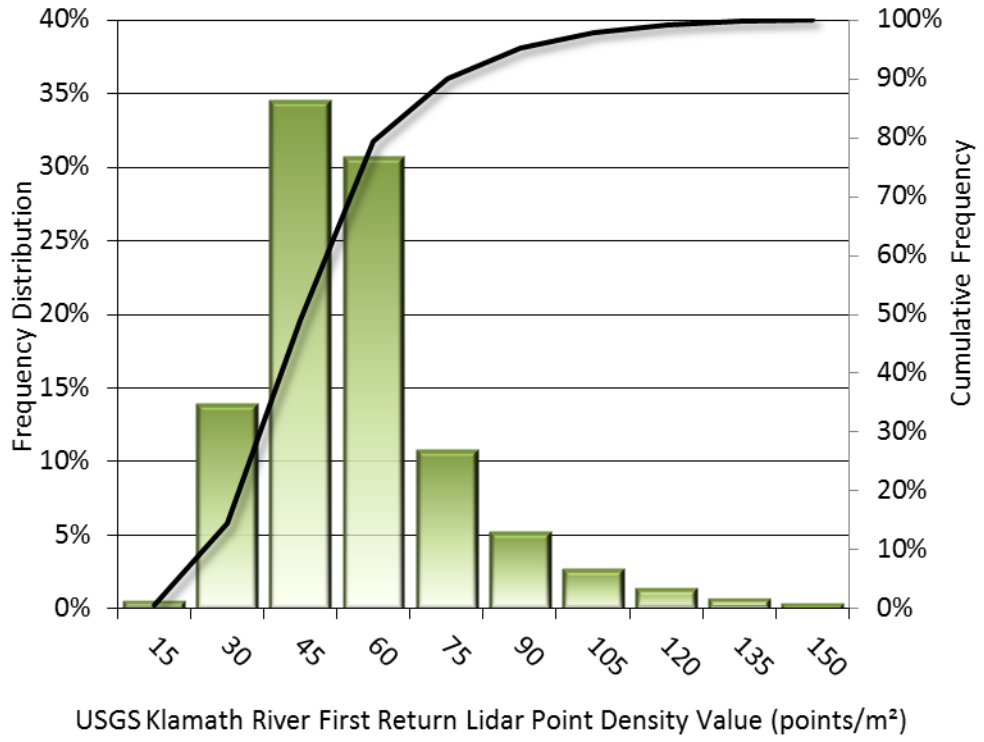


Figure 8: Frequency distribution of first return densities per 100 x 100 m cell

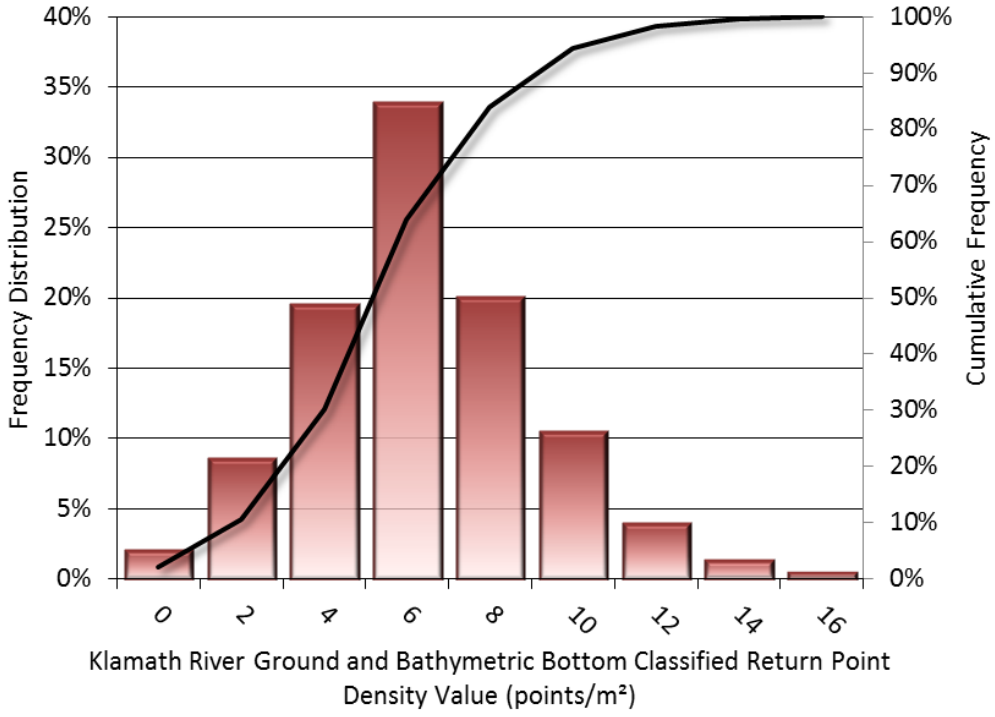


Figure 9: Frequency distribution of ground and bathymetric bottom classified return densities per 100 x 100 m cell

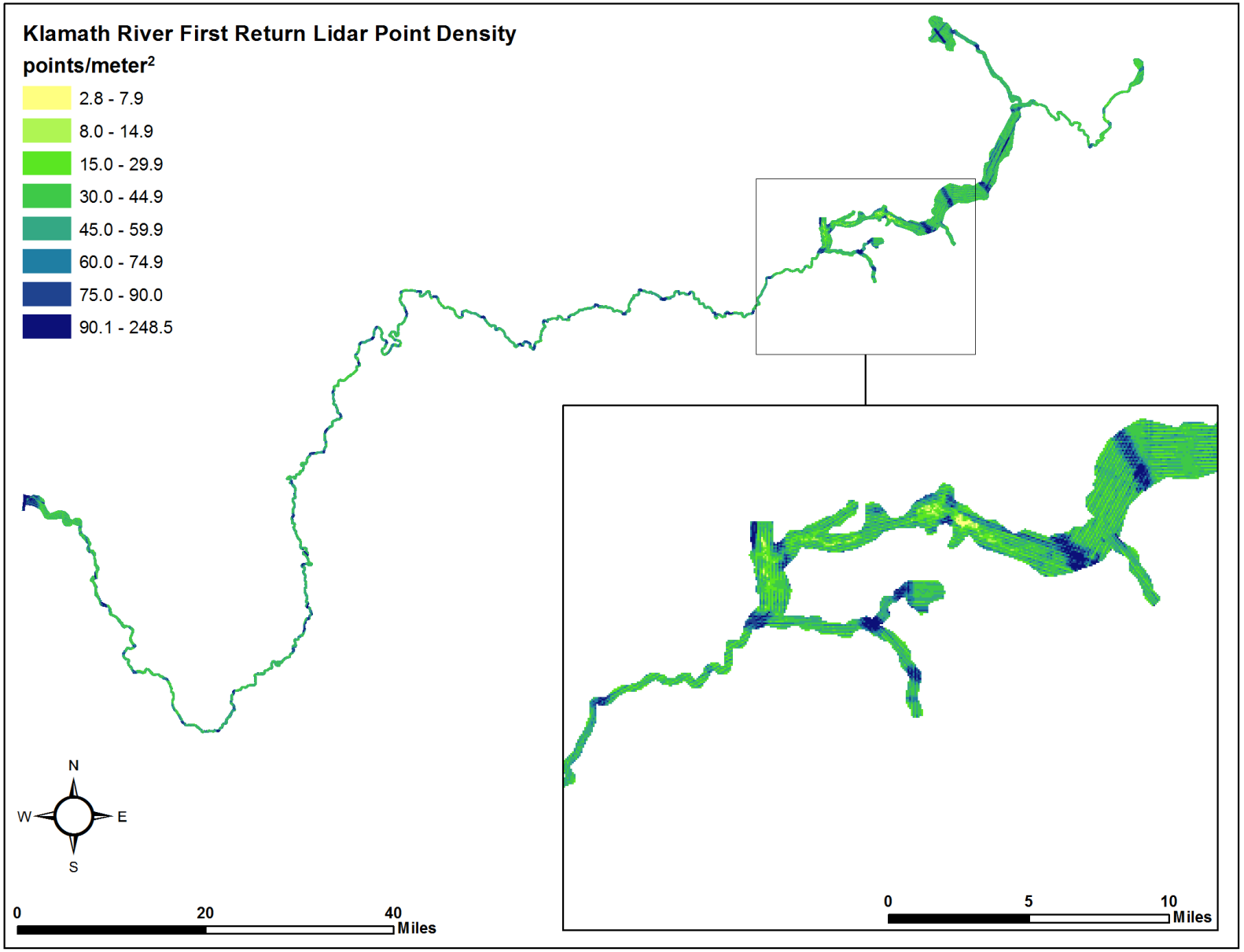


Figure 10: First return Lidar point density map for the Klamath River site (100 m x 100 m cells)

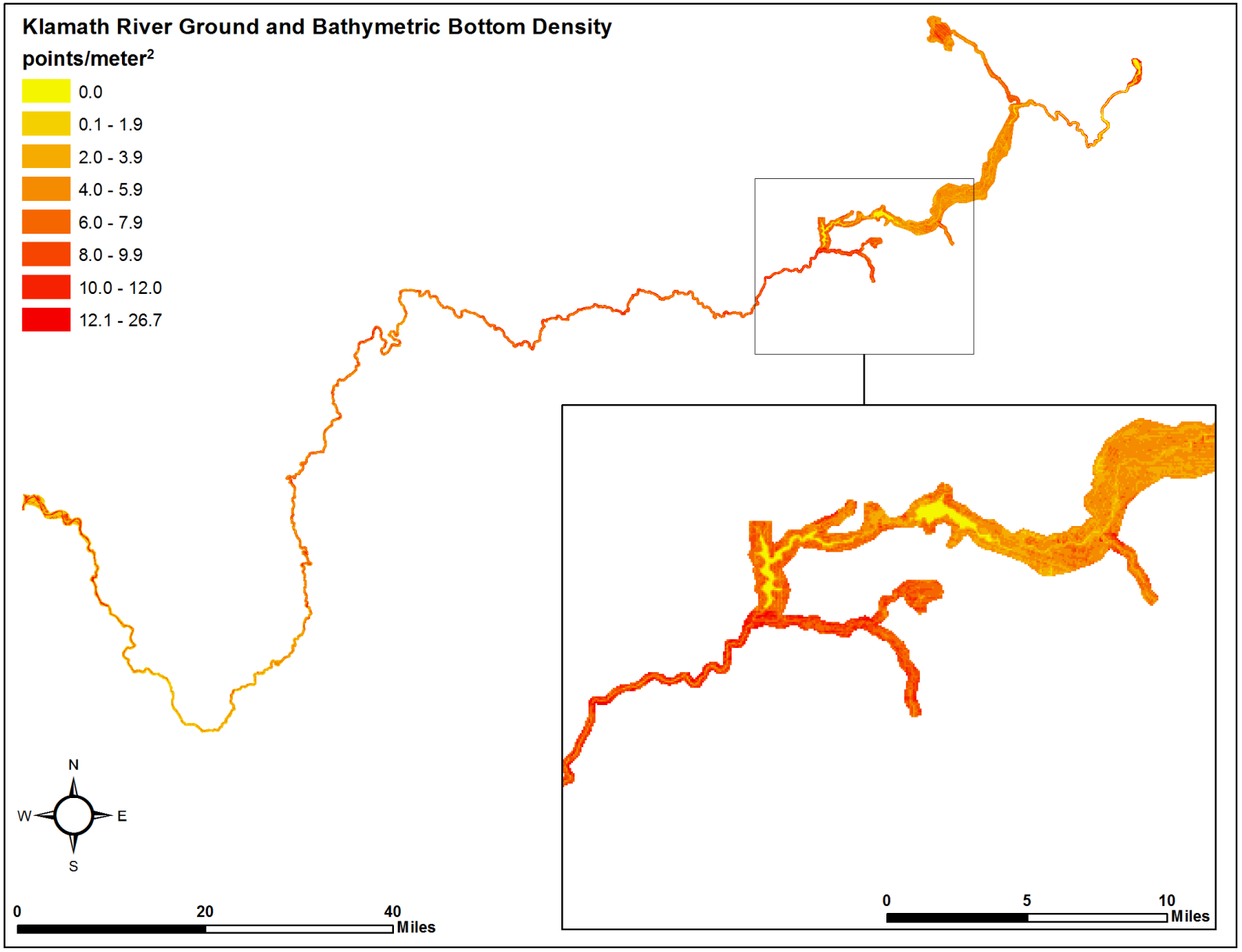


Figure 11: LiDAR-derived Ground and bathymetric bottom density map for the Klamath River site (100 m x 100 m cells)

Lidar Accuracy Assessments

The accuracy of the lidar data collection can be described in terms of absolute accuracy (the consistency of the data with external data sources) and relative accuracy (the consistency of the dataset with itself). See Appendix A for further information on sources of error and operational measures used to improve relative accuracy.

Lidar Non-Vegetated Vertical Accuracy

Absolute accuracy was assessed using Non-vegetated Vertical Accuracy (NVA) reporting designed to meet guidelines presented in the FGDC National Standard for Spatial Data Accuracy[2]. NVA compares known ground quality assurance point data collected on open, bare earth surfaces with level slope (<20°) to the triangulated surface generated by the unclassified lidar point cloud as well as the derived gridded bare earth DEM. NVA is a measure of the accuracy of lidar point data in open areas where the lidar system has a high probability of measuring the ground surface and is evaluated at the 95% confidence interval (1.96 * RMSE), as shown in Table 17.

The mean and standard deviation (sigma σ) of divergence of the ground surface model from ground check point coordinates are also considered during accuracy assessment. These statistics assume the error for x, y and z is normally distributed, and therefore the skew and kurtosis of distributions are also considered when evaluating error statistics. For the Klamath River survey, 21 ground check points were collected over non-vegetated surfaces, with resulting non-vegetated vertical accuracy of 0.074 meters, as compared to the unclassified LAS and 0.080 meters against the bare earth DEM, with 95% confidence (Figure 12 and Figure 13).

QSI also assessed absolute accuracy using 901 ground control points. Although these points were used in the calibration and post-processing of the lidar point cloud, they still provide a good indication of the overall accuracy of the lidar dataset, and therefore have been provided in Table 17 and Figure 14.

[2] Federal Geographic Data Committee, ASPRS POSITIONAL ACCURACY STANDARDS FOR DIGITAL GEOSPATIAL DATA EDITION 1, Version 1.0, NOVEMBER 2014. http://www.asprs.org/PAD-Division/ASPRS-POSITIONAL-ACCURACY-STANDARDS-FOR-DIGITAL-GEOSPATIAL-DATA.html.

Table 17: Absolute accuracy (NVA) results

Absolute Vertical Accuracy			
	NVA - Ground Check Points (LAS)	**NVA - Ground Check Points (DEM)**	**Ground Control Points**
Sample	21 points	21 points	901 points
95% Confidence (1.96*RMSE)	0.074 m	0.080 m	0.059 m
Average	-0.002 m	-0.005 m	-0.015 m
Median	0.001 m	-0.003 m	-0.015 m
RMSE	0.038 m	0.041 m	0.030 m
Standard Deviation (1σ)	0.039 m	0.042 m	0.026 m

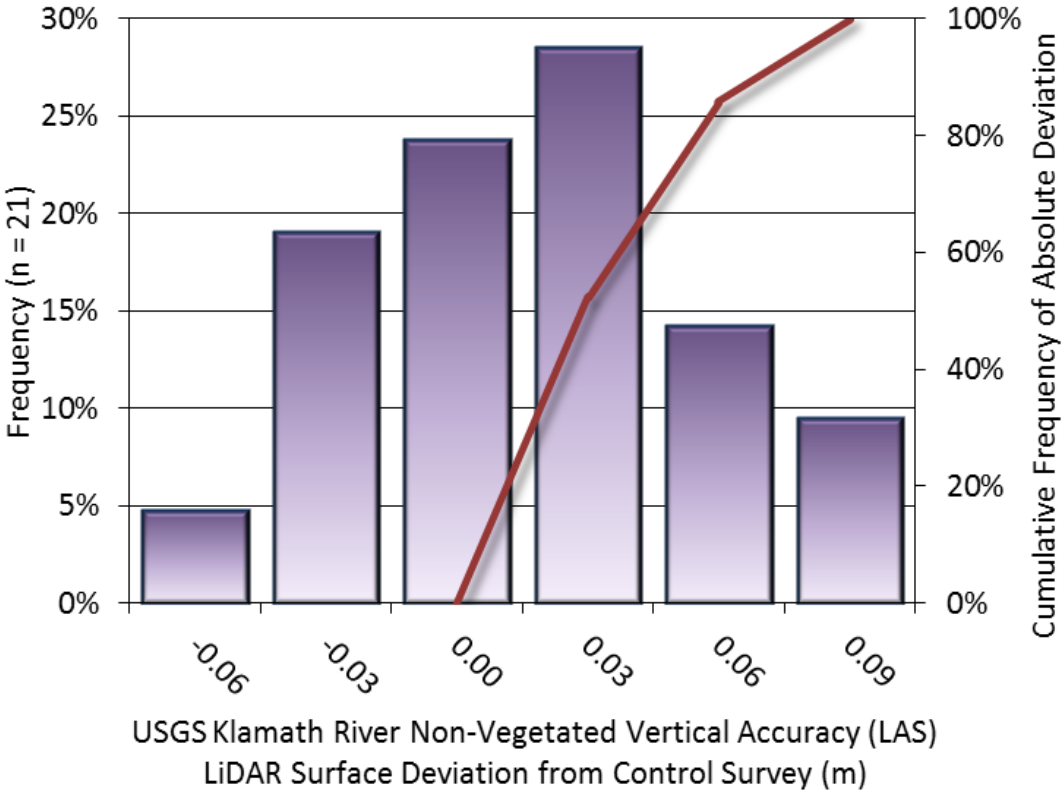


Figure 12: Frequency histogram for lidar surface deviation from ground check point values as compared to the unclassified point cloud

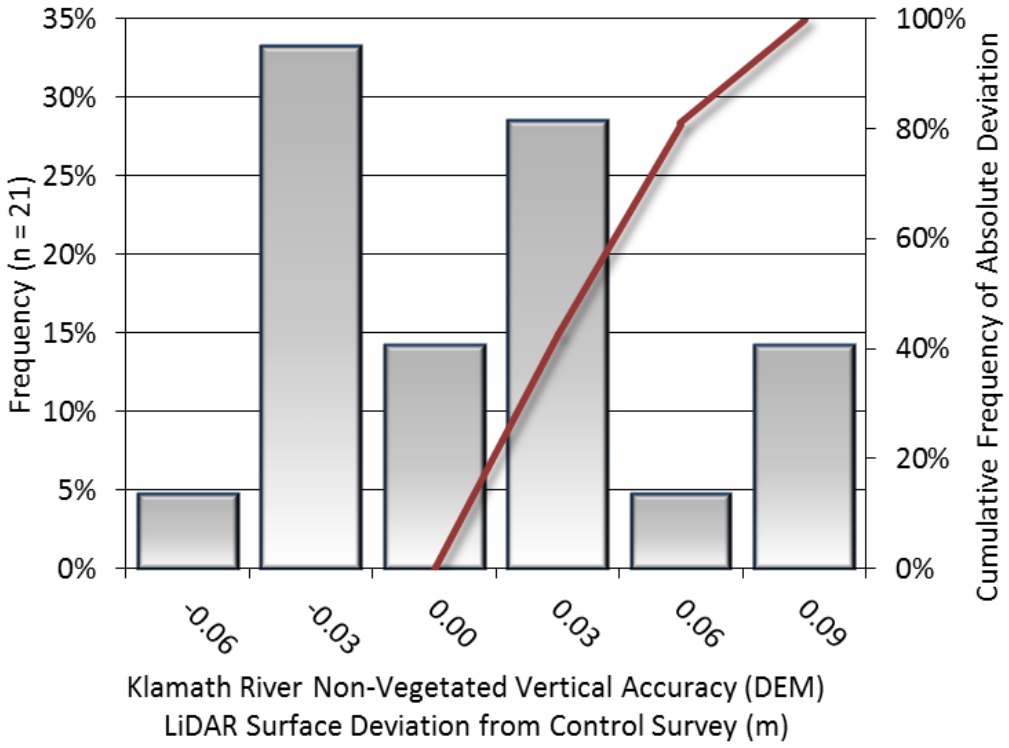


Figure 13: Frequency histogram for lidar surface deviation from ground check point values as compared to the bare earth digital elevation model

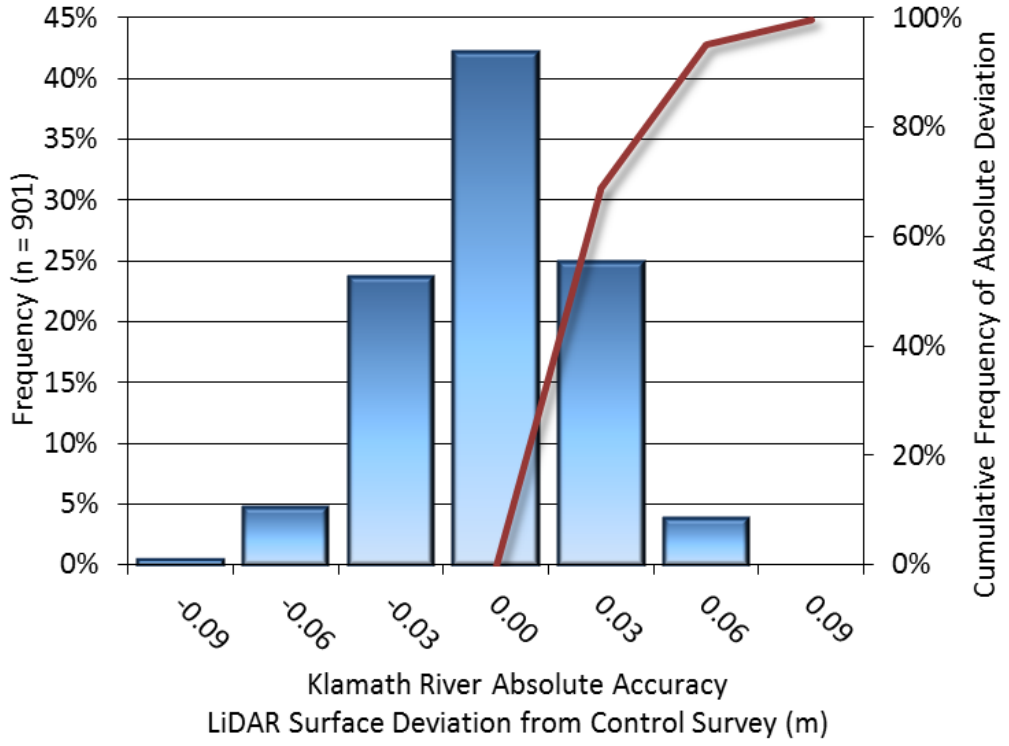


Figure 14: Frequency histogram for lidar surface deviation ground control point values

Lidar Vegetated Vertical Accuracies

QSI also assessed vertical accuracy using Vegetated Vertical Accuracy (VVA) reporting. VVA compares known ground check point data collected over vegetated surfaces using land class descriptions. Check points are compared to the gridded bare earth surface DEM generated by the ground classified lidar points. VVA is evaluated at the 95th percentile. For the Klamath River survey, 9 ground check points were collected over vegetated surfaces, with resulting vegetated vertical accuracy of 0.163 meters at the 95th percentile as compared to the gridded bare earth surface. (Table 18, Figure 15).

Table 18: Vegetated Vertical Accuracy for the Klamath River Project

Vegetated Vertical Accuracy (VVA)	
Sample	9 points
Average Dz	0.071 m
Median	0.075 m
RMSE	0.103 m
Standard Deviation (1σ)	0.079 m
95th Percentile	0.163 m

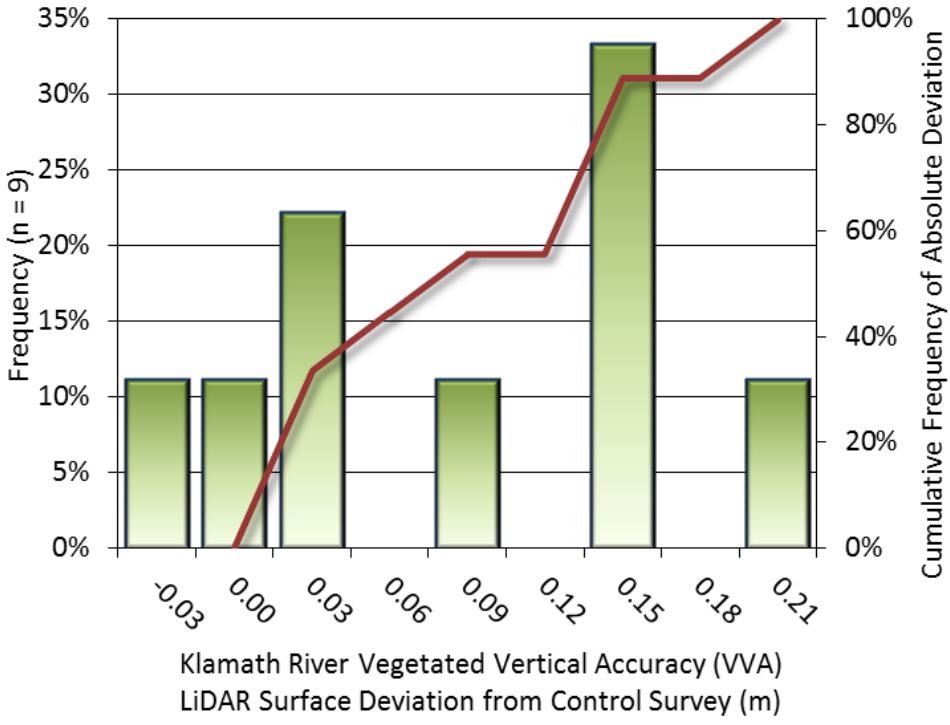


Figure 15: Frequency histogram for lidar surface deviation from all land cover class point values (VVA)

Lidar Bathymetric Vertical Accuracies

Bathymetric (submerged or along the water's edge) check points were also collected in order to assess the submerged surface vertical accuracy. Assessment of the bathymetric checkpoints was performed against the triangulated surface generated by the bathymetric lidar point cloud. Assessment of 103 submerged bathymetric check points resulted in a vertical accuracy of 0.089 meters, while assessment of 78 wetted edge check points resulted in a vertical accuracy of 0.085 meters, with 95% confidence (Figure 16 and Figure 17). Table 19 below presents bathymetric accuracy results and also includes summary statistics for the submerged bathymetric check points at various depth ranges.

Table 19: Bathymetric Vertical Accuracy

Bathymetric Vertical Accuracy for Check Points at Indicated Depth							
	Submerged Check Points						Wetted Edge Check Points
	0 – 0.25 m	0.25 – 0.5 m	0.5 – 0.75 m	0.75 – 1.0 m	> 1.0 m	Cumulative	
Sample	17 points	28 points	31 points	22 points	5 points	103 points	78 points
Average DZ	-0.031 m	-0.011 m	0.003 m	0.001 m	0.024 m	-0.006 m	-0.005 m
Median	-0.032 m	-0.021 m	-0.011 m	-0.019 m	0.013 m	-0.019 m	-0.006 m
RMSE	0.048 m	0.040 m	0.043 m	0.052 m	0.049 m	0.045 m	0.043 m
Standard Deviation (1σ)	0.037 m	0.039 m	0.043 m	0.053 m	0.047 m	0.045 m	0.043 m
95% confidence	0.093 m	0.079 m	0.084 m	0.102 m	0.095 m	0.089 m	0.085 m

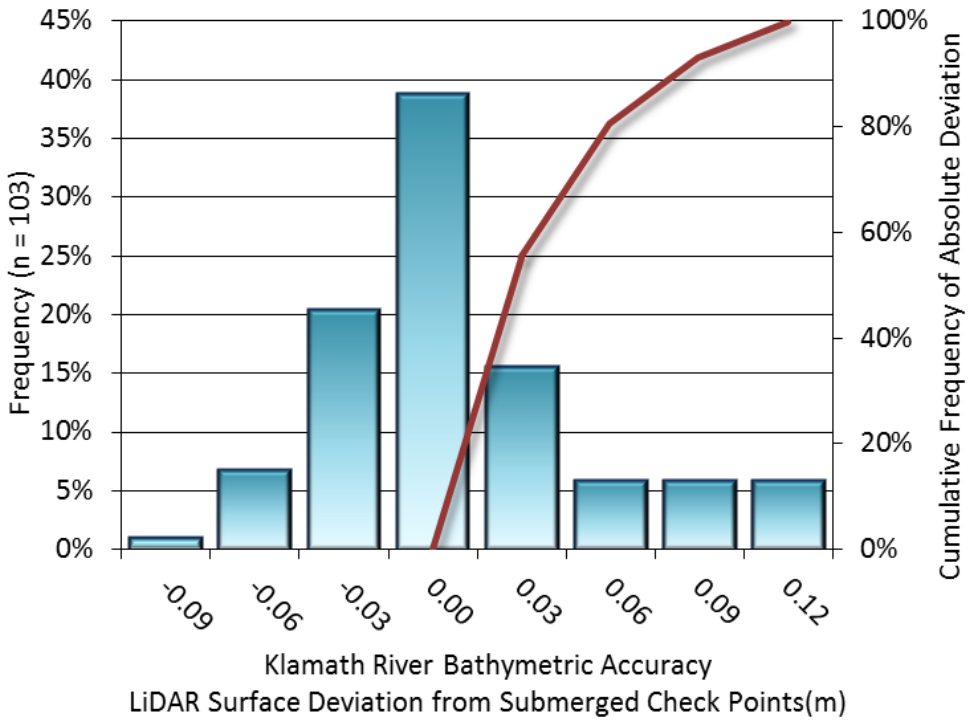


Figure 16: Frequency histogram for lidar surface deviation from bathymetric check point values

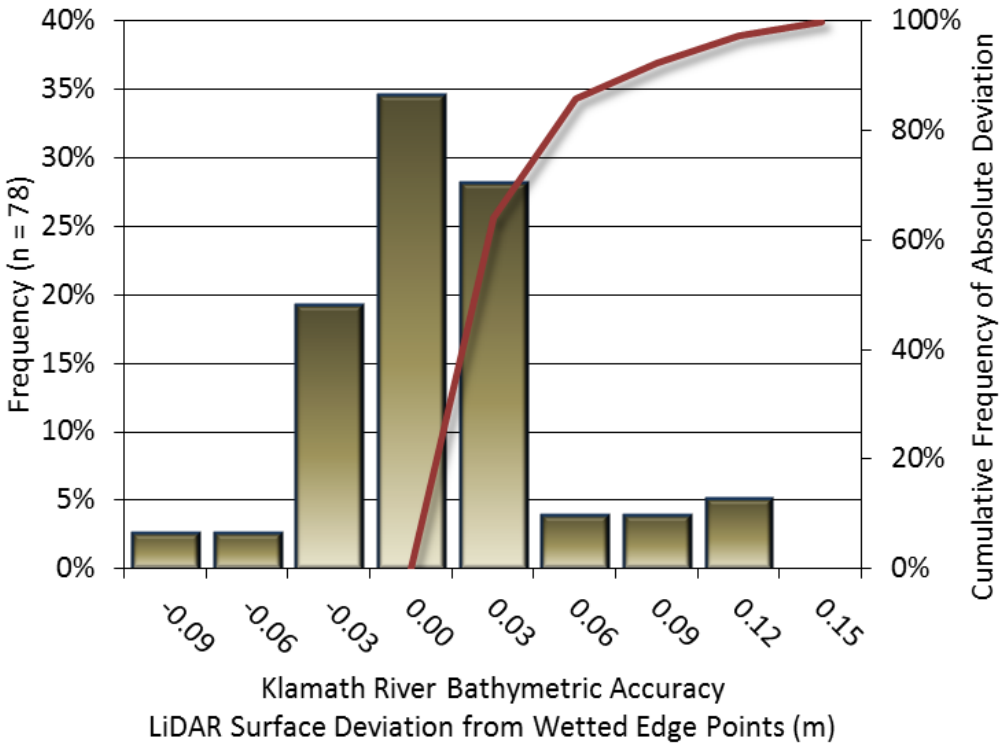


Figure 17: Frequency histogram for lidar surface deviation from wetted edge check point values

Lidar Relative Vertical Accuracy

Relative vertical accuracy refers to the internal consistency of the data set as a whole: the ability to place an object in the same location given multiple flight lines, GPS conditions, and aircraft attitudes. When the lidar system is well calibrated, the swath-to-swath vertical divergence is low (<0.10 meters). The relative vertical accuracy was computed by comparing the ground surface model of each individual flight line with its neighbors in overlapping regions. The average (mean) line to line relative vertical accuracy for the Klamath River lidar project was 0.045 meters (Table 20, Figure 18).

Table 20: Relative accuracy results

Relative Accuracy	
Sample	1,328 surfaces
Average	0.045 m
Median	0.046 m
RMSE	0.050 m
Standard Deviation (1σ)	0.014 m
1.96σ	0.028 m

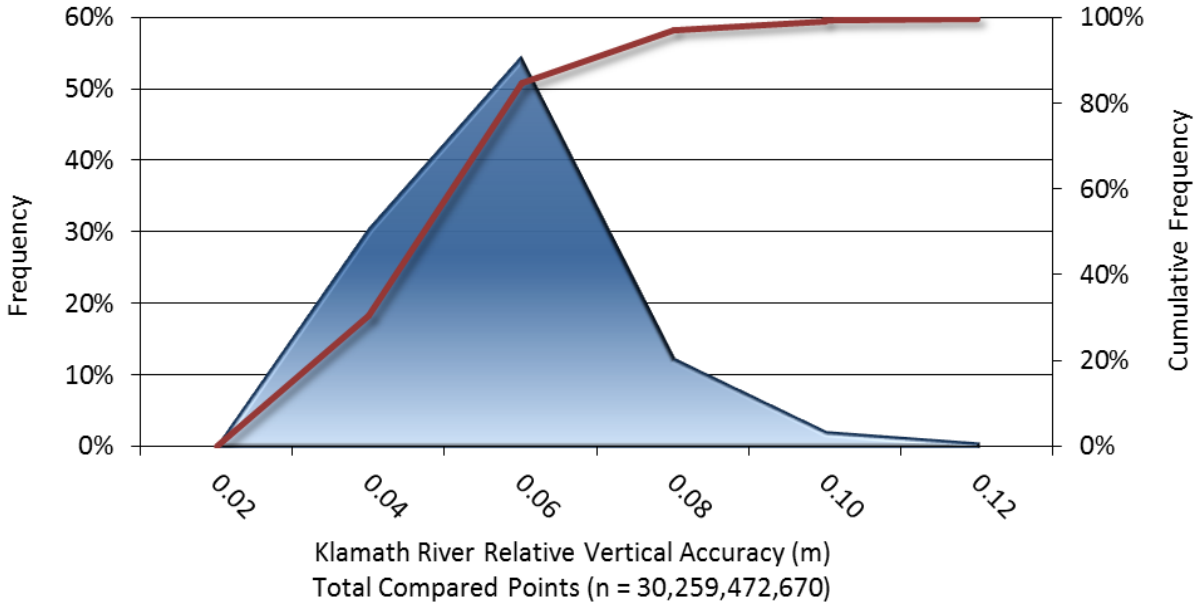


Figure 18: Frequency plot for relative vertical accuracy between flight lines

Digital Imagery Accuracy Assessment

Image accuracy was measured by independent air target check points withheld from the aerial triangulation procedure. Check points were identified in the orthophotos and the displacement was recorded for further statistical analysis.

The circular standard error (CSE) for the Klamath River site is 0.102 meters; the circular standard error was approximated based on the FGDC National Standard for Spatial Data Accuracy (NSSDA) for horizontal accuracy[3]. The CSE (at 95% standard) was computed as follows:

where $RMSE_x = RMSE_y$: $CSE = 1.7308 * RMSE_{xy}$

Table 21 presents the complete photo accuracy statistics.

Table 21: Orthophotography accuracy statistics for Klamath River

Klamath River Photo Accuracy				
		Check Points$_x$	Check Points$_y$	Check Points$_{xy}$
Count		n = 21		
Mean	*m*	0.005	0.044	0.045
RMSE	*m*	0.070	0.072	0.100
1σ	*m*	0.071	0.058	0.092
1.96σ	*m*	0.140	0.114	0.180

[3] Federal Geographic Data Committee, Geospatial Positioning Accuracy Standards (FGDC-STD-007.3-1998). Part 3: National Standard for Spatial Data Accuracy, Appendix 3-A, page 3-10. http://www.fgdc.gov/standards/projects/FGDC-standards-projects/accuracy/part3/chapter3

Analytical Aerial Triangulation Report

Overview

Aerotriangulation was performed in one block to support photogrammetric mapping efforts of the Klamath River. The block consisted of 67 flight lines and 1,781 images flown at a scale of 1:1,200 between June 8 and 23, 2018 (Figure 19). Adjustments were made to ground control established by QSI and GMA referencing UTM Zone 10N, NAD83(2011) horizontal datum and NAVD 1988 vertical datum (Geoid12b). Digital imagery along with ground control and camera calibration data were used as input to Inpho's Match AT softcopy photogrammetry program. The digital cameras utilized were an UltraCam XP and and UltraCam Falcon. Of the 121 total surveyed air target points, 48 were used for aerial triangulation, 21 were withheld from the block adjustment as check points for accuracy assessment and 52 were designated as extraneous because of close proximity to neighboring air target points. Extraneous points are ATPs surveyed over the same ground feature, for example of the four ATPs surveyed at each corner of a stop bar only one would be used for control purposes. This redundancy helps when reviewing the orthos during QAQC and serves as a failsafe in the case that a ground control point fails precision requirements.

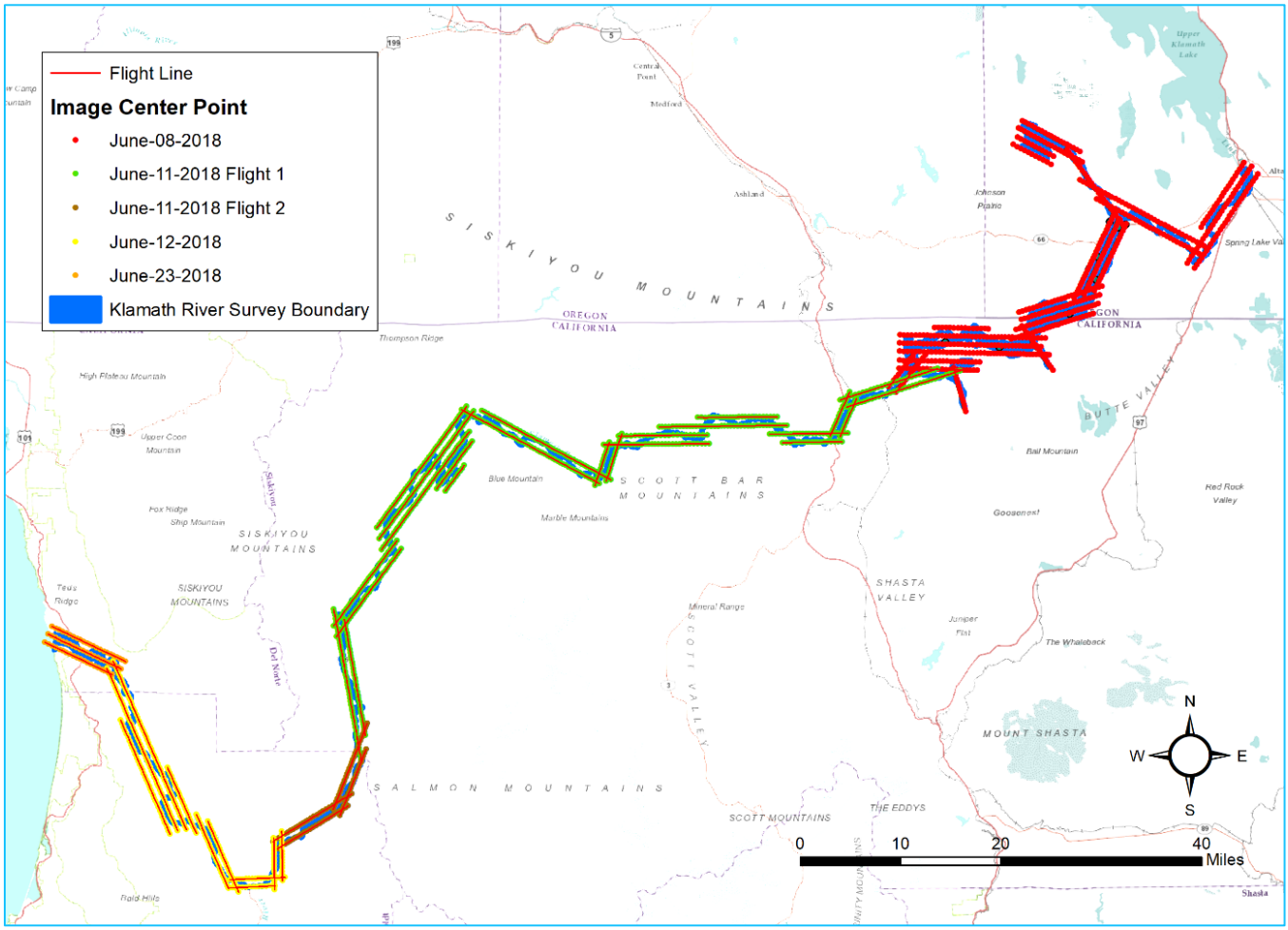


Figure 19: Klamath River photo flight diagram

Control Points

Air target points used in the aerial triangulation adjustment are listed with their coordinates and residuals in Table 22, RMSE values can be found in Table 23.

Table 22: Location and residuals of air target points used as control for aerial triangulation adjustment

Control Point Coordinates - 48 Total Points				Control Point Residuals		
Point ID	X (m)	Y (m)	Z (m)	X (m)	Y (m)	Z (m)
1075	580246.483	4665354.503	1161.097	-0.030	-0.067	-0.084
1093	581392.132	4665817.716	1187.552	0.007	0.004	-0.033
5009	561156.585	4646145.287	798.080	-0.023	0.035	0.144
5026	572365.872	4651530.767	1028.460	0.025	-0.043	0.004
5027	576569.545	4656941.306	1288.734	0.046	0.005	0.230
5335	552415.234	4646994.637	718.935	-0.026	0.002	-0.204
AT002	599071.311	4667696.294	1248.811	-0.003	0.019	-0.028
AT004	591891.242	4658742.964	1265.171	-0.019	-0.020	0.252
AT007	575374.421	4670901.206	1258.952	-0.004	0.016	0.008
AT008	573228.852	4677395.865	1385.610	0.017	0.000	0.119
AT009	565319.538	4681951.869	1518.179	-0.006	0.019	0.062
AT014	552871.665	4641977.710	817.752	0.023	-0.054	-0.205
AT016	544750.245	4640776.959	661.250	0.089	0.009	-0.208
AT017	540734.504	4638593.410	658.662	-0.008	0.043	0.239
AT022	525441.937	4633423.212	581.357	-0.019	0.011	0.088
AT023	521730.135	4635102.013	567.099	0.022	-0.013	0.052
AT025	512495.447	4631521.269	532.292	0.003	-0.064	-0.112
AT027	500218.475	4630225.762	493.948	0.021	0.016	-0.076
AT028	497008.546	4625078.904	478.125	-0.001	-0.007	-0.147
AT030	490387.774	4628693.847	454.955	-0.010	-0.018	0.159
AT032	483547.580	4632357.392	417.449	-0.016	0.005	0.036
AT033	474363.123	4634108.597	383.205	-0.018	0.030	-0.055
AT034	472092.659	4627258.100	532.925	0.023	-0.021	0.006
AT037	463544.929	4619188.517	306.006	-0.010	0.020	-0.042
AT038	462519.358	4612294.688	280.743	-0.010	-0.001	0.004
AT040	455386.776	4602482.205	237.672	0.015	0.018	-0.100
AT041	456110.131	4597462.614	223.363	-0.013	-0.022	0.069
AT043	459159.267	4581173.715	202.519	0.005	0.010	0.035
AT044	456393.420	4573572.360	180.134	-0.007	0.005	-0.067
AT046	444942.081	4565484.052	122.927	0.043	0.026	-0.017
AT047	444052.501	4561069.860	116.054	0.023	-0.003	-0.062
AT049	431385.575	4570153.846	65.817	0.019	-0.010	-0.185
AT050	435335.010	4566485.469	100.528	-0.010	0.011	-0.168
AT052	417500.811	4595810.800	21.706	0.010	0.021	-0.213
AT055	411580.803	4601415.413	7.829	-0.003	0.001	-0.075

Control Point Coordinates - 48 Total Points				Control Point Residuals		
Point ID	X (m)	Y (m)	Z (m)	X (m)	Y (m)	Z (m)
AT057	508727.111	4632525.991	515.498	0.019	0.041	-0.025
AT058	555117.892	4644532.126	946.111	-0.045	0.027	0.080
AT003_QA	592835.228	4666303.697	1259.790	-0.008	-0.006	-0.145
AT005_QA	588623.635	4664689.633	1252.052	0.001	0.013	-0.041
AT017_QA	540736.572	4638599.999	658.501	-0.213	0.057	0.212
AT024_QA	515133.107	4635371.713	541.525	-0.040	0.007	0.120
AT029_QA	469028.988	4627934.606	350.803	0.000	-0.004	0.005
AT062_QA	533920.008	4631235.505	630.637	-0.044	-0.063	0.020
AT064_QA	536101.690	4638883.225	686.085	0.313	0.009	-0.186
AT065_QA	538026.537	4638582.116	650.273	-0.130	-0.025	0.057
AT069_QA	596905.761	4664028.129	1247.222	0.008	0.002	0.065
AT071_QA	600195.096	4671848.831	1257.494	-0.012	-0.014	-0.138
AT072_QA	600620.188	4675057.391	1246.444	0.015	0.006	0.349

Table 23: RMSE for air target points used as control for aerial triangulation adjustment

Control Point RMSE - 48 Total Points		
meters		
X	Y	Z
0.062	0.027	0.132

Check Points

Air target check points withheld from the aerial triangulation adjustment are listed with their coordinates and residuals in Table 24, RMSE values can be found in Table 25.

Table 24: Location and residuals of air target check points withheld from aerial triangulation adjustment

Check Point Coordinates - 21 Total Points				Check Point Residuals		
Point ID	X (m)	Y (m)	Z (m)	X (m)	Y (m)	Z (m)
1076	580244.841	4665370.441	1160.651	0.018	0.052	-0.122
1079	578849.379	4666257.977	1175.755	-0.077	0.006	-0.192
5000	576792.358	4660636.165	1021.605	0.134	-0.133	0.273
AT001	600186.965	4674919.461	1247.069	0.013	0.055	0.397
AT015	546271.121	4642338.107	669.109	0.082	-0.022	-0.463
AT020	535477.504	4633740.482	630.503	-0.098	-0.158	-0.034
AT021	531653.584	4631401.972	608.771	-0.175	-0.072	0.118
AT024	515117.153	4635367.644	541.726	-0.047	0.127	0.171
AT026	502924.637	4630194.929	501.561	0.069	0.109	-0.140
AT035	468403.961	4626575.651	333.763	0.018	-0.033	0.008
AT039	458715.150	4607100.629	260.670	0.074	-0.026	-0.142

Check Point Coordinates - 21 Total Points				Check Point Residuals		
Point ID	X (m)	Y (m)	Z (m)	X (m)	Y (m)	Z (m)
AT051	428702.727	4574749.439	67.775	0.071	0.101	-0.490
AT054	413363.330	4598025.829	13.209	0.111	-0.101	-0.575
AT020_QA	535468.364	4633745.537	630.727	-0.131	-0.155	-0.065
AT035_QA	468401.353	4626576.875	333.586	-0.070	-0.021	-0.118
AT036_QA	468773.808	4627537.369	351.861	-0.070	0.036	-0.174
AT059_QA	468841.193	4627388.338	351.681	0.081	0.011	-0.154
AT060_QA	535367.015	4633787.623	631.614	-0.083	-0.079	-0.054
AT061_QA	535361.853	4633783.398	631.859	-0.024	-0.211	-0.057
AT068_QA	539626.172	4638509.520	648.417	-0.112	-0.082	0.286
AT070_QA	595231.229	4666776.222	1247.040	-0.030	-0.001	-0.013

Table 25: RMSE for air target points withheld from aerial triangulation adjustment

Check Point RMSE - 21 Total Points		
meters		
X	Y	Z
0.086	0.095	0.250

Adjusted Exterior Orientation Parameters

The refined camera position and attitude parameters for each image event can be found in the provided Klamath_River_Photo_Flight_Index.xlsx deliverable.

CERTIFICATIONS

Quantum Spatial, Inc. provided lidar services for the Klamath River project as described in this report.

I, Steve Miller, have reviewed the attached report for completeness and hereby state that it is a complete and accurate report of this project.

Sep 6, 2019

Steve Miller
Project Manager
Quantum Spatial, Inc.

I, Evon P. Silvia, PLS, being duly registered as a Professional Land Surveyor in and by the states of Oregon and California, hereby certify that the methodologies, static GNSS occupations used during airborne flights, and ground survey point collection were performed using commonly accepted Standard Practices. QSI field work conducted for this report was conducted between May 30 and June 12, 2018.

Accuracy statistics shown in the Accuracy Section of this Report have been reviewed by me and found to meet the "National Standard for Spatial Data Accuracy".

REGISTERED
PROFESSIONAL
LAND SURVEYOR

OREGON
JUNE 10, 2014
EVON P. SILVIA
81104LS

EXPIRES: 06/30/2020

LICENSED LAND SURVEYOR
EVON PETER SILVIA
9401
STATE OF CALIFORNIA

Signed: Sep 6, 2019

Evon P. Silvia, PLS
Quantum Spatial, Inc.
Corvallis, OR 97330

Figure 20: View of Klamath River near Teneyck Creek, the shaded bare-earth and topobathymetric model and above ground lidar point cloud are draped with 0.15 m ortho imagery.

Figure 21: A view looking north along the Klamath River in northern California. This image was created from the lidar bare earth model colored by elevation and overlaid with digital imagery acquired by QSI.

GLOSSARY

1-sigma (σ) Absolute Deviation: Value for which the data are within one standard deviation (approximately 68th percentile) of a normally distributed data set.

1.96 * RMSE Absolute Deviation: Value for which the data are within two standard deviations (approximately 95th percentile) of a normally distributed data set, based on the FGDC standards for Non-vegetated Vertical Accuracy (FVA) reporting.

Accuracy: The statistical comparison between known (surveyed) points and laser points. Typically measured as the standard deviation (sigma σ) and root mean square error (RMSE).

> **Absolute Accuracy:** The vertical accuracy of lidar data is described as the mean and standard deviation (sigma σ) of divergence of lidar point coordinates from ground survey point coordinates. To provide a sense of the model predictive power of the dataset, the root mean square error (RMSE) for vertical accuracy is also provided. These statistics assume the error distributions for x, y and z are normally distributed, and thus we also consider the skew and kurtosis of distributions when evaluating error statistics.
>
> **Relative Accuracy:** Relative accuracy refers to the internal consistency of the data set; i.e., the ability to place a laser point in the same location over multiple flight lines, GPS conditions and aircraft attitudes. Affected by system attitude offsets, scale and GPS/IMU drift, internal consistency is measured as the divergence between points from different flight lines within an overlapping area. Divergence is most apparent when flight lines are opposing. When the lidar system is well calibrated, the line-to-line divergence is low (<10 cm).
>
> **Root Mean Square Error (RMSE):** A statistic used to approximate the difference between real-world points and the lidar points. It is calculated by squaring all the values, then taking the average of the squares and taking the square root of the average.

Data Density: A common measure of lidar resolution, measured as points per square meter.

Digital Elevation Model (DEM): File or database made from surveyed points, containing elevation points over a contiguous area. Digital terrain models (DTM) and digital surface models (DSM) are types of DEMs. DTMs consist solely of the bare earth surface (ground points), while DSMs include information about all surfaces, including vegetation and man-made structures.

Intensity Values: The peak power ratio of the laser return to the emitted laser, calculated as a function of surface reflectivity.

Nadir: A single point or locus of points on the surface of the earth directly below a sensor as it progresses along its flight line.

Overlap: The area shared between flight lines, typically measured in percent. 100% overlap is essential to ensure complete coverage and reduce laser shadows.

Pulse Rate (PR): The rate at which laser pulses are emitted from the sensor; typically measured in thousands of pulses per second (kHz).

Pulse Returns: For every laser pulse emitted, the number of wave forms (i.e., echoes) reflected back to the sensor. Portions of the wave form that return first are the highest element in multi-tiered surfaces such as vegetation. Portions of the wave form that return last are the lowest element in multi-tiered surfaces.

Real-Time Kinematic (RTK) Survey: A type of surveying conducted with a GPS base station deployed over a known monument with a radio connection to a GPS rover. Both the base station and rover receive differential GPS data and the baseline correction is solved between the two. This type of ground survey is accurate to 1.5 cm or less.

Post-Processed Kinematic (PPK) Survey: GPS surveying is conducted with a GPS rover collecting concurrently with a GPS base station set up over a known monument. Differential corrections and precisions for the GNSS baselines are computed and applied after the fact during processing. This type of ground survey is accurate to 1.5 cm or less.

Scan Angle: The angle from nadir to the edge of the scan, measured in degrees. Laser point accuracy typically decreases as scan angles increase.

Native Lidar Density: The number of pulses emitted by the lidar system, commonly expressed as pulses per square meter.

Relative Accuracy Calibration Methodology:

Manual System Calibration: Calibration procedures for each mission require solving geometric relationships that relate measured swath-to-swath deviations to misalignments of system attitude parameters. Corrected scale, pitch, roll and heading offsets were calculated and applied to resolve misalignments. The raw divergence between lines was computed after the manual calibration was completed and reported for each survey area.

Automated Attitude Calibration: All data were tested and calibrated using TerraMatch automated sampling routines. Ground points were classified for each individual flight line and used for line-to-line testing. System misalignment offsets (pitch, roll and heading) and scale were solved for each individual mission and applied to respective mission datasets. The data from each mission were then blended when imported together to form the entire area of interest.

Automated Z Calibration: Ground points per line were used to calculate the vertical divergence between lines caused by vertical GPS drift. Automated Z calibration was the final step employed for relative accuracy calibration.

Lidar accuracy error sources and solutions:

Type of Error	Source	Post Processing Solution
GPS (Static/Kinematic)	Long Base Lines	None
	Poor Satellite Constellation	None
	Poor Antenna Visibility	Reduce Visibility Mask
Relative Accuracy	Poor System Calibration	Recalibrate IMU and sensor offsets/settings
	Inaccurate System	None
Laser Noise	Poor Laser Timing	None
	Poor Laser Reception	None
	Poor Laser Power	None
	Irregular Laser Shape	None

Operational measures taken to improve relative accuracy:

Low Flight Altitude: Terrain following was employed to maintain a constant above ground level (AGL). Laser horizontal errors are a function of flight altitude above ground (about 1/3000th AGL flight altitude).

Focus Laser Power at narrow beam footprint: A laser return must be received by the system above a power threshold to accurately record a measurement. The strength of the laser return (i.e., intensity) is a function of laser emission power, laser footprint, flight altitude and the reflectivity of the target. While surface reflectivity cannot be controlled, laser power can be increased and low flight altitudes can be maintained.

Reduced Scan Angle: Edge-of-scan data can become inaccurate. The scan angle was reduced to a maximum of ±20^{o} from nadir, creating a narrow swath width and greatly reducing laser shadows from trees and buildings.

Quality GPS: Flights took place during optimal GPS conditions (e.g., 6 or more satellites and PDOP [Position Dilution of Precision] less than 3.0). Before each flight, the PDOP was determined for the survey day. During all flight times, a dual frequency DGPS base station recording at 1 second epochs was utilized and a maximum baseline length between the aircraft and the control points was less than 13 nm at all times.

Ground Survey: Ground survey point accuracy (<1.5 cm RMSE) occurs during optimal PDOP ranges and targets a minimal baseline distance of 4 miles between GPS rover and base. Robust statistics are, in part, a function of sample size (n) and distribution. Ground survey points are distributed to the extent possible throughout multiple flight lines and across the survey area.

50% Side-Lap (100% Overlap): Overlapping areas are optimized for relative accuracy testing. Laser shadowing is minimized to help increase target acquisition from multiple scan angles. Ideally, with a 50% side-lap, the nadir portion of one flight line coincides with the swath edge portion of overlapping flight lines. A minimum of 50% side-lap with terrain-followed acquisition prevents data gaps.

Opposing Flight Lines: All overlapping flight lines have opposing directions. Pitch, roll and heading errors are amplified by a factor of two relative to the adjacent flight line(s), making misalignments easier to detect and resolve.

THIS PAGE INTENTIONALLY LEFT BLANK

2018 KLAMATH DAM REMOVAL PROJECT
TOPOBATHYMETRIC LIDAR & SONAR
TECHNICAL DATA REPORT

AECOM Project Number 60537920

Prepared for:

AECOM
300 Lakeside Drive, Suite 400
Oakland, CA 94612

Prepared by:

Cort Pryor

GMA Hydrology, Inc. (GMA)
5435 Ericson Way, Suite 1
Arcata, CA 95521
(707) 825-6681

December, 2018





Table of Contents

EXECUTIVE SUMMARY 1
SURVEYOR'S STATEMENT 1
INTRODUCTION 2
Survey Area 2
DATA ACQUISITION 4
Geodetic Control 4
LiDAR Surveys 4
Sonar Surveys 4
Multibeam Surveys 6
Sweep Sonar Surveys 6
Ground Surveys 7
Topography 7
Ground Survey Check Points 7
DATA PROCESSING 7
Geodetic Control 7
Topo-Bathymetric LiDAR 8
Multibeam and Sweep Sonar 8
Ground Surveys 10
Data Integration and Product Development 10
Deliverables 13
RESULTS AND DISCUSSION 14
No Data Areas 14
ACCURACY ASSESSMENT 14
Absolute Vertical Accuracy 14
Topo-Bathymetric LiDAR 14
Multibeam and Sweep Sonar 14
REFERENCES 16
APPENDICES A-1

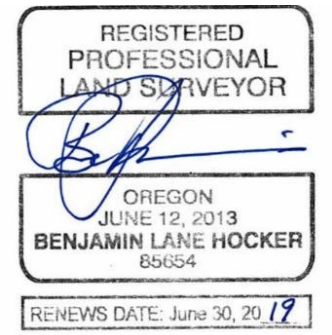
EXECUTIVE SUMMARY

In support of the Klamath Hydroelectric Settlement Agreement (KHSA), four PacifiCorp hydropower facilities located in the Klamath River Basin (Iron Gate Dam, Copco No. 1 Dam, Copco No. 2 Dam and J.C. Boyle Dam) were surveyed using topo-bathymetric airborne LiDAR, multibeam sonar, sweep sonar and conventional methods.

This report summarizes the geodetic control, data collection techniques, processing and data integration methodologies, as well as the assessed accuracy of the datasets.

SURVEYOR'S STATEMENT

I, Benjamin L. Hocker as a licensed land surveyor in the state of Oregon (No. 85654), certify that the airborne LiDAR, multibeam sonar, sweep sonar and terrestrial control survey data within Oregon compiled by GMA Hydrology, Inc. in partnership with Geomatics Data Solutions, Inc. follows commonly accepted standard practices. Accuracy statistics shown were tested to meet a 0.61 (ft) $RMSE_z$ Vertical Accuracy Class based on ASPRS Positional Accuracy Standards for Digital Geospatial Data (2014). The 2018 Klamath River Survey Report (GMA Hydrology, Inc., 2018) documents data collection methods, processing, and data integration methods.



I, David T. Edson as a licensed land surveyor in the state of California (No. 4974), certify that the airborne LiDAR, multibeam sonar, sweep sonar and terrestrial control survey data within California compiled by GMA Hydrology, Inc. in partnership with Geomatics Data Solutions, Inc. follows commonly accepted standard practices. Accuracy statistics shown were tested to meet a 0.61 (ft) $RMSE_z$ Vertical Accuracy Class based on ASPRS Positional Accuracy Standards for Digital Geospatial Data (2014). The 2018 Klamath River Survey Report (GMA Hydrology, Inc., 2018) documents data collection methods, processing, and data integration methods.



12/3/2018

INTRODUCTION

Survey Area

The project area includes the Klamath River and four reservoirs that straddle the Oregon and California border: John C. Boyle Reservoir located in southern Oregon near the township of Keno and Copco 1, Copco 2 and Iron Gate Reservoirs in Siskiyou County, California (Figure 1).

GMA Hydrology, Inc. (GMA) and Geomatics Data Solutions, Inc. (GDS) performed all terrestrial and hydrographic surveys. Airborne surveys were conducted by Quantum Spatial, Inc. (QSI) under contract with GMA.

Data acquisition occurred between February 08, 2018 and August 09, 2018. Acquisition dates and area surveyed, according to survey source, are show in Table 1.

Table 1. Acquisition Dates and Area Surveyed

Data Type	Survey Area (sq km)	Acquisition Dates
LiDAR	108	June 11 through June 13, 2018
Bathymetric LiDAR	1.27	June 11 through June 13, 2018
Multibeam	7.59	February 8, 2018 through 8-Aug-18
Sweep	0.56	May 9-10 & 29-30, 2018
GNSS RTK	0.001	August 9, 2018

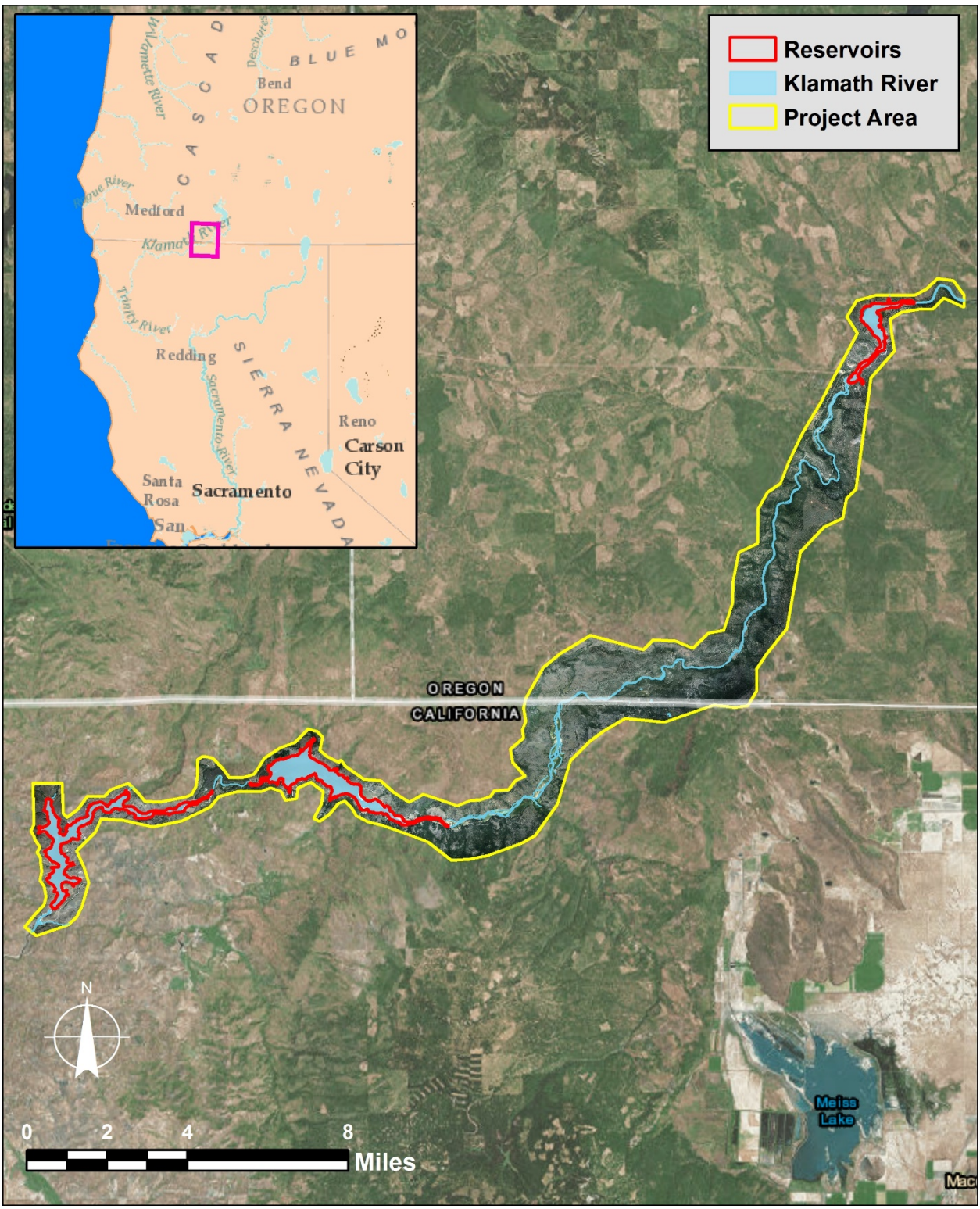


Figure 1. Klamath River Survey Area Overview

DATA ACQUISITION

Equipment specifications can be found in Appendix B.

Geodetic Control

GMA and GDS established five new control stations and occupied 8 existing stations in the survey area using static Global Navigation Satellite Systems (GNSS) network survey techniques. Trimble R10 and R8 model 3 GNSS receivers were configured to record raw multiple frequency, multiple constellation observables at a rate of 1 Hz. Multiple observations with independent baselines were obtained between existing published NGS control, recovered control from previous LiDAR and imagery projects, and newly set monumentation. Fixed height tripods were used to minimize antenna setup errors. QSI utilized two additional monuments for conducting airborne data acquisition.

The horizontal datum is NAD83 (2011) Epoch 2010.0 and the vertical datum is NAVD88 using GEOID12B. Data are projected in Universal Transverse Mercator, Zone 10 in meters (m).

LiDAR Surveys

QSI was contracted by GMA to collect topo-bathymetric Light Detection and Ranging (LiDAR) data and digital imagery. The LiDAR survey was accomplished using a Riegl VQ-880-G green laser system mounted in a Bell 206L-3 Rotorcraft. Full details on LIDAR acquisition is described in *Klamath_Reservoirs_Topobathymetric_LiDAR_Report – signed,* submitted under a separate cover.

Sonar Surveys

GMA and GDS worked in partnership to conduct bathymetric surveys at the four reservoir sites. Two vessels and four sonar systems were utilized during survey operations, as detailed in Table 2.

GDS-Cari (Figure 2) and GMA-Jet are both aluminum hull jet boats fitted with over the side pole mounted multibeam sonar systems. GMA- Jet was also configured with a Ross Laboratories 875-8 portable hydrographic sonar sweep system (Figure 3).

Table 2: Sonar Systems

Survey Area	Vessel	Major Components
John C Boyle	GDS-Cari GMA-Jet	Reson SeaBat T20-P Multibeam Ross 875 8-Channel Sweep
Copco 1	GMA-Jet GDS-Cari	Reson SeaBat T20-P Multibeam Reson SeaBat T20-P Multibeam
Copco 2	GMA-Jet	Norbit iWBMS STX Multibeam
Iron Gate	GMA-Jet GDS-Cari	Norbit iWBMSc Multibeam Reson SeaBat T20-P Multibeam



Figure 2. GDS-Cari Configured with Pole Mounted Reson T20-P Multibeam Sonar



Figure 3. GMA-Jet Configured with Ross 875-8 Sweep Sonar

Multibeam Surveys

The multibeam sonar surveys were conducted with a Reson SeaBat T20-P and two different versions of the Norbit iWBMS sonar system. The systems were deployed on the GDS Cari platform well as the GMA Jet boat. Applanix POS/MV inertial navigation systems were used to position and orient the sonar data with auxiliary Trimble R10 and R8 model 3 GNSS receivers for positioning system redundancy and QA/QC. The sonar, inertial, and positioning data were stored on an on-board computer running Applanix and Teledyne PDS survey software. A shore-based Trimble R8 Model 3 GNSS receiver broadcasted Real Time Kinematic (RTK) GNSS positioning corrections to the survey vessels via UHF radio link (Figure 4). Raw GNSS observables were also recorded at the base and vessel for post-processing. Surface sound speed was measured at the sonar head during acquisition by an AML sound speed probe. Sound speed profiles were measured over the full depth of the project area using an AML MinosX profiler.

Proper system operation was calibrated and verified using industry standard position checks, bar checks and patch tests. Crosslines were also collected to verify sonar accuracy and provide an independent check for LiDAR and sweep data.

Sweep Sonar Surveys

The sonar sweep survey was conducted using a portable multi-channel sonar sweep system. The GMA jet boat was equipped with a Ross Laboratories 875-8 portable hydrographic sonar sweep system, Trimble SPS852/552H GNSS receiver heading bundle, and a Honeywell HMR 3000 attitude sensor. A shore-based Trimble R8 Model 3 GNSS receiver broadcasted Real Time Kinematic (RTK) GNSS positioning corrections to the survey vessels via UHF radio link (Figure 4). Raw GNSS observables were also recorded at the base and vessel for post-processing. The sonar data, RTK GNSS data, and attitude data were combined in a ruggedized laptop computer running Hypack hydrographic surveying software. Sound speed profiles were acquired using a YSI CastAway CTD and an AML BaseX.



Figure 4. GNSS Base Station

The control points used for sonar surveys at each reservoir are presented in Table 3.

Table 3. Control Coordinates on NAD83 (2011) Epoch 2010.0

Control Point	Latitude	Longitude	Ellipsoid Height (m)	Survey Area
GMA-200	N42°07'21.97179"	W122°02'52.79449"	1136.533	John C Boyle Reservoir
GMA-202	N41°58'25.76728"	W122°17'55.95491"	772.760	Copco Reservoirs
GMA-203	N41°57'50.65426"	W122°25'49.06258"	731.917	Iron Gate Reservoir

Ground Surveys

Topography

Ground topographic surveys were performed in areas where sonar and topo-bathymetric LiDAR acquisition were not possible. The topographic survey area consisted of a small region of the Copco 2 reservoir about 70 meters downstream of the Copco No. 1 dam. The survey was conducted using Trimble R8 Model 3 and R10 receivers.

Ground Survey Check Points

GMA, GDS, and QSI collected ground survey check points (GSCP) using RTK, post-processed kinematic (PPK) and fast-static (FS) survey techniques. Multiple frequency, survey grade Trimble GNSS receivers were used as base and rovers for all surveys (models R10, R8-2, R8-3, and R7). Base station receivers were setup on control monuments to broadcast a kinematic correction to rover receivers as well as record raw observables for post-processing. In General GSCP measurements were made during periods with a Position Dilution of Precision (PDOP) of ≤ 3.0 with at least six satellites in view of the stationary and roving receivers. When collecting RTK and PPK data, the rover records data while stationary for five seconds, then calculates the pseudorange position using at least three one-second epochs. FS surveys record observations for up to fifteen minutes on each GSCP in order to support longer baselines for post-processing. Relative errors for any GSCP position must be less than 1.5 cm horizontal and 2.0 cm vertical in order to be accepted.

GSCPs were collected in areas where good satellite visibility was achieved on varying surface types and slopes. GSCPs were distributed over the project area, however distribution of GSCPs depended on ground access constraints and monument locations and may not be equitably distributed throughout the study area.

DATA PROCESSING

Geodetic Control

Raw GNSS observables were post processed with precise ephemeris files in Trimble Business Center version 4.00 software. A constrained least squares adjustment was performed to determine final coordinates. Coordinates for all monuments are shown in Appendix A-1.

Topo-Bathymetric LiDAR

Upon completion of data acquisition, QSI processing staff initiated a suite of automated and manual techniques to process the data into the requested deliverables. Processing tasks included GNSS control computations, smoothed best estimate trajectory (SBET) calculations, kinematic corrections, calculation of laser point position, sensor and data calibration for optimal relative and absolute accuracy, and LIDAR point classification.

Riegl's RiProcess software was used to facilitate bathymetric return processing. Once bathymetric points were differentiated, they were spatially corrected for refraction through the water column based on the angle of incidence of the laser. QSI refracted water column points using QSI's proprietary LAS processing software, LAS Monkey. The resulting point cloud data were classified using both manual and automated techniques. Processing methodologies were tailored for the landscape.

Full details on LIDAR processing is described in *Klamath_Reservoirs_Topobathymetric_LiDAR_Report – signed,* submitted under a separate cover.

Multibeam and Sweep Sonar

Once sonar data collection was complete, GMA processed all sonar data in Caris HIPS version 10. Processing is a combination of manual and automated techniques that are tailored to the deliverables requested by the client. Processing steps included: defining vessel configurations, SBET calculations, converting raw Hypack and PDS data files to HIPS format, applying sound velocity corrections, reviewing and correcting attitude and navigation data, review and editing of raw sounding data, manual and automated filtering as well as merging the attitude, navigation and raw sounding data. Post-processed trajectory from POSPac was applied to enhance positional accuracy and compute Total Propagated Uncertainty (TPU). For multibeam and sweep sonar data, the processed track lines were binned using a Bathymetry Associated with Statistical Error (BASE) Surface type. Multibeam sonar data was binned using the Combined Uncertainty and Bathymetry Estimator (CUBE) algorithm using 25cm resolution. Sweep sonar data was binned using the CUBE algorithm with a 75 cm resolution. Sonar processing workflow is presented in Table 4.

Table 4. Sweep and Multibeam Beam Sonar Processing Workflow

Sonar Processing Step	Software Used
Define vessel configuration for the survey. Configuration includes sensor types and models, location of sensors, lever arms, and uncertainties associates with measurements.	Caris HIPS 10.4.2
Convert raw sonar files to HIPS format. Each survey line is converted separately and stored by day.	Caris HIPS 10.4.2
Import delayed heave, SBET and RMS.	Caris HIPS 10.4.2 POSPac 8.2.6633.20855
Apply sound velocity corrections, review navigation, heading, GNSS water levels, and attitude data.	Caris HIPS 10.4.2
Merge processed soundings with navigation, attitude, and GNSS water levels.	Caris HIPS 10.4.2
Generate CUBE surface and continue processing point cloud in subsets. Automated and manual filtered using the surface as a reference.	Caris HIPS 10.4.7
Export final point cloud by survey line for all crosslines and perform various accuracy assessments.	Caris HIPS 10.4.7 ArcMap 10.6 Microsoft Excel
Export CUBE surface resampled on Klamath Reservoirs Index to ASCII.	Caris HIPS 10.4.7

Relative vertical confidence checks of the multibeam sonar were completed using crosslines and bar checks. Each bar check was conclusive with differences generally 1cm or less. Crosslines acquired throughout the project area were analyzed in Caris HIPS by creating difference surfaces. 25cm resolution CUBE surfaces of the crosslines were subtracted from 25cm resolution surfaces of the main scheme lines for each reservoir (Table 5). Crossline results were reviewed for across-track bias errors (roll offset, speed of sound errors, etc.), gross error (GNSS height), and total vertical uncertainty (TVU).

Table 5. Klamath River Reservoirs Crossline Comparisons

Surface Differencing	
Minimum	-1.788 m
Maximum	0.940 m
Mean	0.005 m
Standard Deviation	0.048 m
Total Count	4,623,618

Significant man-made features were flagged during data processing to ensure the gridded surfaces would represent those least depths (Figure 5).

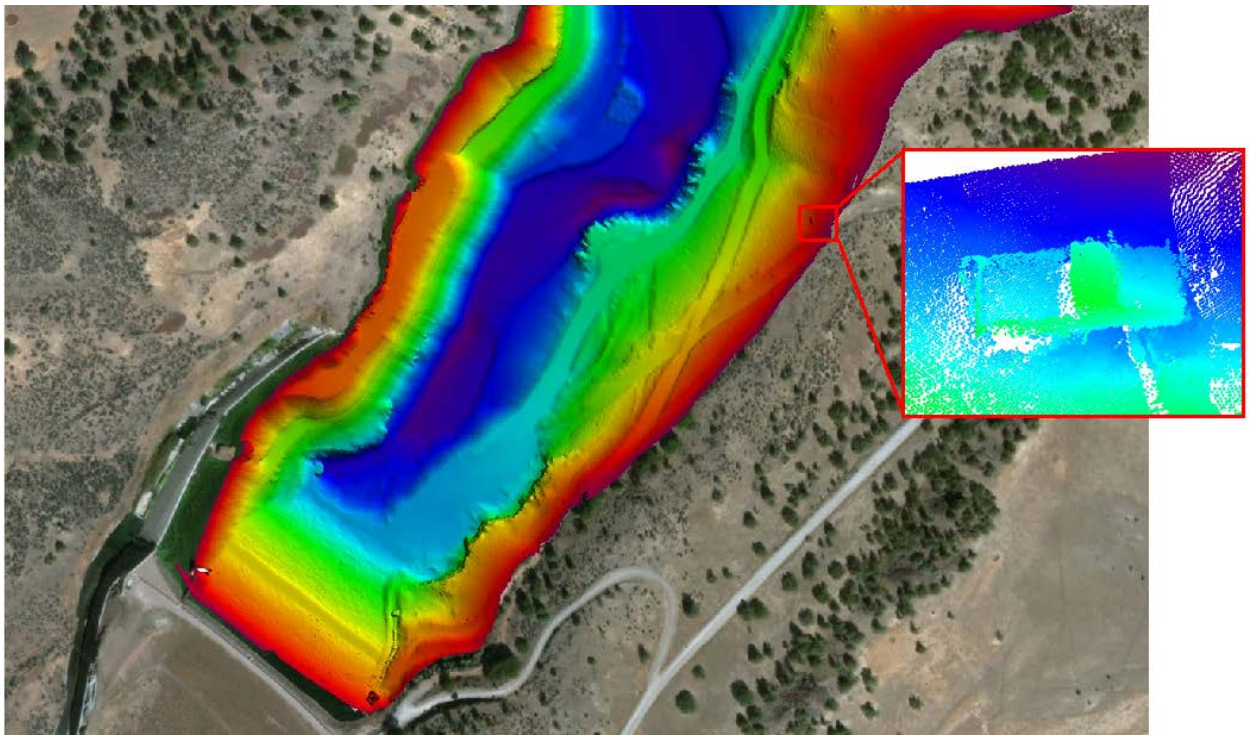


Figure 5. Truck Located in High Resolution Multibeam at Iron Gate Reservoir

Ground Surveys

Topographic and ground survey check point data were processed in Trimble Business Center version 4.00 software. Processing included: verifying values for geodetic control, verifying and modifying rod heights, verifying and modifying point codes, sorting the data to various layers and developing feature breaklines.

Data Integration and Product Development

The multibeam sonar, sweep sonar and topo-bathymetric LiDAR data were integrated using GeoCue's LP360 4.4 and ArcMap 10.6. Integration of the data sets included, converting survey data to *.LAS format, updating point classifications (Table 6), developing survey extents by data

Table 6: LAS File Point Classification

Classification Number	Classification Name	Classification Description
1	Default/ Unclassified	Flightline edge clip
2	Ground	Laser returns that are determined to be ground using automated and manual cleaning algorithms
3	Low Vegetation	Vegetation between 0.25 and 2 meters
4	Medium Vegetation	Vegetation between 2 and 5 meters
5	High Vegetation	Vegetation above 5 meters
7	Noise	Scattering points and artificial points below the ground surface
9	NIR Water Surface	NIR laser returns that are determined to be water using automated and manual cleaning algorithms
17	Bridge	Bridge Decks
40	Bathy LiDAR	Laser returns determined to be ground within the a wetted region
41	Green Water Surface	Green laser returns that are determined to be water surface points using automated and manual cleaning algorithms
45	Water Column	Refracted Riegl sensor returns that are determined to be water using automated and manual cleaning algorithms
71	GNSS RTK	Ground Survey points that were collected with RTK GPS
80	Sweep Sonar Binned	Binned sonar returns that were collected with a multi-transducer sonar sweep system
81	Multibeam Sonar Binned	Binned sonar returns that were collected with a multibeam sonar system

type, developing buffers for sonar and conventional datasets, developing breaklines, determining absolute accuracy of the dataset, and developing client requested deliverables. The integration and product development workflow is described in Table 7.

Table 7: Data Integration Workflow

Data Integration Step	Description
Convert and classify data	Convert ASCII files to *.las v1.4 PDRF 6. Classify data based on source.
Survey/Data Extents	Develop individual data and survey extents. Develop project extents.
Terrain Development and Inspection	Develop terrain using appropriate point classifications, add withheld flag to appropriate classes in areas of overlapping data, apply breaklines developed during conventional survey data processing, and contour. Add additional breaklines to force correct interpolation of features. Visually inspect terrain for correct interpolation, additional data flagging and breakline development as needed.
Data Accuracy Assessment	Query the terrain dataset with GSCPs. Develop statistics according to ASPRS Positional Accuracy Standards for Digital Geospatial Data (Edition 1, Version 1.0. – November 2014)
Final Products	Develop and review final products requested by client

Deliverables

The deliverables provided for Klamath survey project are shown in Table 8. The deliverables are provided electronically and can be found on the portable hard disk accompanying this report.

Table 8: Survey Data Deliverables

Electronic Data Deliverables	
Point Cloud Data Package	Point Cloud (*.las) and Tiled ● Topographic LiDAR Points ● Bathymetric LiDAR Points ● Conventional Points (GNSS RTK) ● Multibeam Sonar (CUBE Algorithm) ● Sweep Sonar (CUBE Algorithm)
Digital Imagery	Full Resolution Data Package ● Tiled Orthorecitfied Image Mosaics (*.tif) ● Ground Control (*.shp) ● Ground Survey Check Points (*.shp) ● Aircraft Position (*.shp) General Use Data Package ● Orthorectified Image Mosaic (*.sid)
Terrain Surface Data Package	Surface Nodes Data Package ● Tiled XYZ Tables of Final Ground Surface Nodes Including Densified Points Derived from Breaklines; ASCII(*.txt) Contour Data Package ● Tiled Seamless Contours (0.5 meter) (*.shp)(*.dxf) Breakline Data Package ● Tiled Seamless Breaklines (*.shp) Terrain Model Data Package ● ArcGIS FileGeodatabase (*.gdb) Raster Data Package ● Half Meter Raster (*.flt)
Terrain Accuracy Data Package	Ground Survey Check Points (*.xlsx) ● Absolute Vertical Accuracy Assessment

RESULTS AND DISCUSSION

No Data Areas

Areas where data were not acquired were left in the terrain model. All significant areas where there are no bathymetric data are identified in the "Klamath_NoDataAreas" Polygons feature class included in the electronic deliverables.

ACCURACY ASSESSMENT

Vertical accuracy assessments are based on the guidelines set forth in the National Standard for Spatial Data Accuracy (NSSDA), (FGDC, 1998) as well as the American Society for Photogrammetry and Remote Sensing (ASPRS, 2014). Absolute accuracy is computed using RMSE statistics in non-vegetated terrain and 95th percentile statistics in vegetated terrain. The aforementioned accuracy standards were developed primarily to describe terrestrial data so it is necessary to extend the meaning of non-vegetated and vegetated when it comes to the bathymetric surface. For the purposes of this accuracy assessment non-vegetated has been extended to include all sonar and conventional survey data collected in relatively flat areas within the wetted channel that contain uniform substrate smaller than the boulder size class and in areas with good water conditions (non-aerated water). Vegetated has been extended to include the remainder of the bathymetric surface; steep slopes non-uniform substrate, boulder and bedrock and aerated water.

Absolute Vertical Accuracy

For the topo-bathymetric LiDAR and sonar datasets, absolute vertical accuracy was assessed using Non-Vegetated Vertical Accuracy (NVA) Reporting. NVA accuracy reporting compares point data collected in areas with open sky, with non-turbulent water conditions, where bed substrate is relatively uniform, a lack of vegetation exists and on surfaces with slopes (<20°) to the triangulated irregular network (TIN) surface generated by the survey data. NVA replaces what was formerly known as Fundamental Vertical Accuracy (FVA) and is a measure of the vertical accuracy of the survey data and is evaluated at the 95% confidence interval.

Topo-Bathymetric LiDAR

GMA and GDS assessed vertical accuracy of the topo-bathymetric LiDAR dataset by collecting 263 independent GSCP's on the topo-LiDAR surface and 4,806 sonar check points on the bathymetric-LiDAR surface. Results are presented in Table 9. An additional 899 sonar check points were collected on the topo-LiDAR surface and are presented for reference (Table 9).

Multibeam and Sweep Sonar

GMA and GDS assessed vertical accuracy of the sonar dataset by collecting sonar crosslines across the main scheme data. Crosslines were primarily collected using multibeam sonar with additional cross lines collected using sweep sonar at the J.C. Boyle reservoir. After nadir beams were extracted from the swath data 35,314 sonar check points were used to assess the accuracy of the multibeam surface and 1,995 points were used to assess the accuracy of the sweep surface. Results are presented in Table 10.

Table 9: Topo-Bathymetric LiDAR Absolute Accuracy (NVA)

Topo-Bathymetric LiDAR Absolute Accuracy			
	Topo LiDAR (GSCP)	**Topo LiDAR (Sonar)**	**Bathymetric LiDAR (Sonar)**
Samples	263 points	899 Points	4,806 Points
Average	0.001 m	0.000 m	-0.006 m
Median	0.002 m	0.000 m	-0.009 m
RMSE	0.035 m	0.066 m	0.052 m
Standard Deviation (1σ)	0.035 m	0.071 m	0.045 m
1.96σ	0.055 m	0.114 m	0.100 m
NVA (1.96*RMSE)	0.069 m	0.129 m	0.101 m

Table 10: Sonar Absolute Accuracy (NVA)

Sonar Absolute Accuracy (NVA)		
	Multibeam Sonar	**Sweep Sonar**
Samples	35,314 Points	1,995 Points
Average	-0.017 m	-0.024 m
Median	-0.016 m	-0.022 m
RMSE	0.048 m	0.070 m
Standard Deviation (1σ)	0.045 m	0.065 m
1.96σ	0.095 m	0.144 m
NVA (1.96*RMSE)	0.094 m	0.136 m

REFERENCES

American Society for Photogrammetry and Remote Sensing, ASPRS Positional Accuracy Standards for Digital Geospatial Data. Edition 1, Version 1, November 2014. http://www.asprs.org/PAD-Division/ASPRS-POSITIONAL-ACCURACY-STANDARDS-FOR-DIGITAL-GEOSPATIAL-DATA.htm

Federal Geographic Data Committee, Geospatial Positioning Accuracy Standards (FGDC-STD-007.3-1998). Part 3: National Standard for Spatial Data Accuracy. http://www.fgdc.gov/standards/projects/FGDC-standards-projects/accuracy/part3/chapter3

Quantum Spatial Inc. Klamath Reservoirs, California and Oregon, Topobathymetric LiDAR Technical Data Report, October 29, 2018

APPENDICES

Appendix A-1: Survey Control Coordinates -- Geographic NAD83(2011) Datum, epoch 2010.00

Monument ID	Latitude (N)	Longitude (W)	Ellipsoid Height (m)	Group	Type	Comment
P380	42° 15' 34.79886"	121° 46' 46.85526"	1391.280	QSI	ORGN RTN	
KLAM_RTK_01	41° 55' 53.60915"	122° 26' 30.05496"	644.842	QSI	Rebar with Cap	
DH6397	N41°53'55.73736"	W122°33'51.85263"	681.022	NGS	Survey Disk	Held
DF9369	N42°11'38.78988"	W121°47'14.54849"	1236.222	NGS	Survey Disk	Held
NZ1016	N42°06'56.74432"	W122°06'53.47462"	1391.879	NGS	Metal Rod	Vertical Check
NZ1023	N42°08'27.91179"	W122°00'43.77427"	1166.120	NGS	Metal Rod	Vertical Check
GMA-200	N42°07'21.97179"	W122°02'52.79449"	1136.533	GMA	Scribe	Adjusted
GMA-201	N42°05'32.08620"	W122°04'20.86394"	995.363	GMA	Rebar with Cap	Adjusted
GMA-202	N41°58'25.76728"	W122°17'55.95491"	772.760	GMA	Rebar with Cap	Adjusted
GMA-203	N41°57'50.65426"	W122°25'49.06258"	731.917	GMA	Rebar with Cap	Adjusted
GMA-205	N41°55'59.62588"	W122°26'03.25854"	727.094	GMA	Rebar with Cap	Adjusted
WCP-101	N41°58'24.42160"	W122°22'02.16531"	696.489	Woolpert	Rebar with Cap	Adjusted
WCP-102	N41°57'51.74165"	W122°15'42.08796"	774.365	Woolpert	Rebar with Cap	Adjusted
WCP-103	N42°00'14.16431"	W122°11'13.78885"	852.313	Woolpert	Rebar with Cap	Adjusted
WCP-104	N42°02'34.29919"	W122°04'53.05303"	1262.654	Woolpert	Rebar with Cap	Adjusted
KR-IGD_DB4	N42°05'46.83442"	W122°02'54.77961"	1246.978	WSI	Rebar	Adjusted

Appendix A-2: Survey Control Coordinates -- Projected
NAD83(2011) Datum, epoch 2010.00
NAVD88 Datum, Geoid 12B
UTM Zone 10, Meters

Monument ID	Northing (Meters)	Easting (Meters)	Elevation (Meters)	Group	Type	Comment
P380	4679328.224	600652.654	1413.923	QSI	ORGN RTN	
KLAM_RTK_01	4642327.954	546288.169	668.682	QSI	Rebar with Cap	
DH6397	4638633.698	536132.198	704.790	NGS	Survey Disk	Held
DF9369	4672039.878	600121.712	1259.037	NGS	Survey Disk	Held
NZ1016	4663008.377	573172.966	1415.089	NGS	Metal Rod	Vertical Check
NZ1023	4665913.277	581630.045	1189.209	NGS	Metal Rod	Vertical Check
GMA-200	4663845.882	578691.141	1159.698	GMA	Scribe	Adjusted
GMA-201	4660434.504	576705.776	1018.612	GMA	Rebar with Cap	Adjusted
GMA-202	4647107.673	558089.338	796.372	GMA	Rebar with Cap	Adjusted
GMA-203	4645943.979	547208.215	755.678	GMA	Rebar with Cap	Adjusted
GMA-205	4642517.562	546904.057	750.933	GMA	Rebar with Cap	Adjusted
WCP-101	4647022.057	552423.239	720.177	Woolpert	Rebar with Cap	Adjusted
WCP-102	4646084.157	561179.265	797.900	Woolpert	Rebar with Cap	Adjusted
WCP-103	4650532.601	567313.273	875.803	Woolpert	Rebar with Cap	Adjusted
WCP-104	4654943.189	576025.236	1285.989	Woolpert	Rebar with Cap	Adjusted
KR-IGD_DB4	4660911.111	578678.238	1270.187	WSI	Rebar	Adjusted

Appendix B-1: Equipment Specifications

GNSS Receiver Specifications	
GNSS Receiver	Trimble R7, R8 Model 3 & R10
Horizontal Accuracy	± 0.003 m + 0.5 ppm RMS (Static Mode) ± 0.008 m + 1 ppm RMS (Kinematic Mode)
Vertical Accuracy	± 0.005 m + 0.5 ppm RMS (Static Mode) ± 0.015 m + 1 ppm RMS (Kinematic Mode)
Initialization time	Typically <10 seconds
Communications	460 MHz Narrow Band

Applanix POS/MV Specifications	
Position Accuracy	0.02 - 0.1 m (RTK)
Heading Resolution	0.03° (RTK) Long Baseline PP (0.08° Short Baseline)
Pitch/Roll Accuracy	0.02° Independent on Baseline
Heave Accuracy	5 cm or 5% (2 cm RTK)

iWBMSc Wideband Multibeam Sonar Settings and Specifications	
Swath Coverage	7-179° (140° Nominal)
Range Resolution	<10 mm (Acoustic)
Number of Beams	256-512 EA & ED
Operating Frequency	400kHz w/ 80kHz Bandwidth (200-700kHz Possible)
Depth Range	0.2-275 m (160 meter typical)
Ping Rate	up to 50Hz, Range Dependent
Resolution	0.9° Across Track, 1.9° Along Track @400kHz

Reason T20-P Multibeam Sonar Settings and Specifications	
Swath Coverage	140° Equi-Distant 165° Equi-Angle
Range Resolution	6 mm
Number of Beams	256-512 EA & ED
Operating Frequency	400kHz w/ 80kHz Bandwidth (190-420kHz frequency agile)
Depth Range	0.5-250 m (150 meter typical)
Ping Rate	up to 50Hz, Range Dependent
Resolution	1° Across Track, 1° Along Track @400kHz

Sweep System Sonar Settings and Specifications		
Transceiver		Ross Labs 875-8
	Output Power	100 watts (RMS)
	Resolution	0.06 ft.
	Pulse Length	0.1 msec
	Ping Rate	55 msec (18.2 Hz)
	Recording Rate	100 msec (10 Hz)
	Minimum Depth	1.5 ft. below transducer face
	Maximum Depth	151 ft. below transducer face
Transducers		Airmar
	Frequency	200 kHz
	Spread	8 degree
Pitch and Roll		Honeywell HMR3000
	Accuracy	±0.4 degrees for Tilt < 20 degrees
Position		Trimble SPS852 GNSS Receiver
	Update Rate	1 Hz to 20 Hz
	Horizontal Accuracy	0.03 ft. + 1 ppm RMS (RTK)
	Vertical Accuracy	0.05 ft. + 1 ppm RMS (RTK)
Heading		Trimble SPS8552H GNSS Receiver
	Update Rate	1 Hz to 20 Hz
	Heading Accuracy	0.09° RMS (2m Antenna Separation)